This thesis is written in the form of a journal article from the International Society for Microbial Ecology

Effects of Temperature on Macromolecular Composition of the Antarctic Diatom, *Corethron pennatum*

Peta L. Vine

Department of Biological Sciences, Macquarie University

Submission date: 25th October 2018

This work has not been submitted for a higher degree to any other university or institution

Declaration

I wish to acknowledge the following assistance in the research detailed in this report:

Dr Philip Heraud, my Adjunct Supervisor, who assisted with method development, spectral analysis and editing my drafts;

Emeritus Professor John Beardall, my Adjunct Supervisor, for assistance with photophysiological analysis and draft editing.

All other research described in this report is my own original work.

Peta L. Vine

Acknowledgements

I would like to thank Dr Philip Heraud for his expert guidance and patience. I would also like to thank Emeritus Professor John Beardall for sharing his wealth of knowledge and guidance. I would also like to extend my appreciation to Associate Professor Grant Hose who gave me the opportunity to conduct this research and made this thesis possible. My sincere thanks also go to Associate Professor Leanne Armand who, without obligation, offered advice and support well beyond the requirements of this research.

I would also like to take this opportunity to thank Dr Yussi Palacios Delgado and Finlay Shanks for their practical and technical support. Lastly, thank you to Miguela Martin, Dale Christensen and Dr David Perez-Guaita for your help with unravelling the mysteries of The Unscrambler.

The author wishes to thank the CSIRO Marine National Facility (MNF) for its support in the form of sea time on *RV Investigator*, support personnel, scientific equipment and data management. All data and samples acquired on the voyage are made publicly available in accordance with MNF Policy. This research was funded by the Australian Government through the Australian Research Council (DP170100557).

Abstract

Southern Ocean temperatures are rising due to climate change. Increasing temperature can alter diatom physiology and survival, subsequently affecting primary productivity and distributions. Diatoms are important primary producers and their composition mediates energy and nutrient transfer to higher trophic levels. Diatom physiology and macromolecular composition are useful indicators for demonstrating and modelling microalgal response to climate change. Using pulse amplitude modulated fluorometry and Attenuated Total Reflectance - Fourier Transform Infrared (ATR-FTIR) spectroscopy, I characterised the physiological response and macromolecular composition of the Antarctic diatom, *Corethron pennatum* cultured at 0 °C to 5°C. The ATR-FTIR generated data were used to create spectroscopy-based predictive models. The photosynthetic capacity of *C. pennatum* decreased as temperatures increased, while all cultures eventually failed at 5 °C. As growth temperature increased, unsaturated fatty acid concentrations generally increased, and protein levels decreased slightly. Lipid levels were lowest at the coldest growth temperatures. These findings, particularly the unusual lipid unsaturation at the highest temperatures, show that *C. pennatum* physiology may differ from many diatoms. Additionally, the model demonstrated a high predictive power (R^2 = 0.98), showing that macromolecular composition of *C. pennatum* is a useful intracellular marker that could be used to model microalgal response to climate change.

Introduction

Aquatic photoautotrophs contribute half of all global primary productivity, supporting marine food webs via oxygenic photosynthesis (1). Microalgae are responsible for most of this primary productivity and 40% is attributed to diatoms (2 and references therein). Diatoms also supply around 20% of global oxygen and remove vast amounts of CO_2 from the atmosphere (3-5). They are also intrinsic to both carbon and silica cycles, particularly in polar environments where diatom abundance is high (6, 7).

Thermal responses of many Antarctic species, particularly microalgae, remain relatively unknown (8). In order to model ecosystem responses to temperature shifts associated with climate change, species-specific data are essential (9, 10). An understanding of acclimation strategies and thermal effects on cell-physiology is important for predicting potential shifts in biogeographical boundaries and function, which can affect food webs and biogeochemical cycles (9, 11). The predicted temperature increases in the Southern Ocean (12, 13) warrant the investigation of the effects of temperature on Antarctic diatoms, particularly as they comprise the base of the food chain (14).

This study aims to demonstrate changes in the growth rate, photosynthetic capacity (photosynthetic efficiency, light harvesting efficiency, relative maximum electron transport rate) and macromolecular composition (protein, lipid and carbohydrate content) of the Antarctic diatom, *Corethron pennatum* in response to different growth temperatures. Additionally, I briefly review the development and use of Attenuated Total Reflectance - Fourier Transform Infrared (ATR-FTIR) spectroscopy (and relevant chemometric methods), to illustrate the potential for its application to studies involving microalgal physiology, particularly within the field of microbial ecology. Additionally, I used spectroscopy-based Partial Least Squares Regression (PLSR) predictive models, to determine whether ATR-FTIR can effectively demonstrate the relationship between diatom physiology and growth temperature.

Effects of climate change on Southern Ocean temperature

Temperatures in regions of the Southern Ocean have risen in recent decades and temperature in the entire Southern Ocean is predicted to rise under climate change. Southern Ocean sub-surface temperatures have risen almost twice as fast as global ocean temperatures over the last 50 years (12). The Antarctic Peninsula has sustained the greatest impact from rapid global climatic warming experienced over the last few decades (15-17). Average summer water temperature near the Western Antarctic Peninsula has risen over 1°C since the 1950s (18); although no statistical change or even weak cooling has occurred in some Southern Ocean regions. Some areas may continue to

cool but others are predicted to increase by an average of 0.03 °C to 0.14 °C per decade (dependent on climate sensitivity) by the end of the century if global CO_2 reduction targets are not met (13). This could have profound effects on Southern Ocean ecosystems.

Effects of temperature on microalgal distribution

Changes in ocean temperature (amongst other factors) directly affect marine ecology and biogeochemistry (19). Thermal regimes can modify community composition and function, as selection favours 'fit' and adaptable phenotypes (20, 21). Temperature tolerance and lethal thresholds potentially define the biogeographic range, or at least the fundamental niche, of microalgae. Evidence of this has been demonstrated in polar, temperate and tropical microalgal strains (17, 22). For example, the growth temperature optima are generally around 6 °C to 8 °C and 22 °C to 24 °C for polar and temperate diatoms respectively (23-26). Additionally, microalgae isolated from different geographical regions can have different thermal ranges (17, 22, 27). The few studies conducted to determine the thermal tolerance of microalgae showed that those isolated from higher latitudes are generally more tolerant of lower temperatures, while lower latitude is associated with higher temperature tolerances. This pattern has been demonstrated in green algae (28, 29), flagellates (30), dinoflagellates (22) and diatoms (17, 25).

Primary production, food webs and biogeochemical cycles

Climate change may already have altered microalgal distributions and food webs in the Western Antarctic Peninsula region. In a 2009 study spanning three decades, a 12% reduction in summer microalgal levels off the Western Antarctic Peninsula corresponded with increasing temperatures observed there (31). Population numbers of Antarctic krill, a key species in the SO, have also been decreasing since the 1970s (18, 32), although this has very recently been questioned (33). A decrease in krill predators, such as the Adélie penguin has also been noted, with increasing numbers of chin strap penguins in their place (31 and references therein). A microalgal assemblage study conducted from 1991 to 1996 observed a switch from diatom to cryptophyte-dominated communities, which are not easily grazed by Antarctic Krill, perhaps explaining the apparent decline in krill populations (34). These occurrences were attributed to sea-ice and meltwater dynamics. However, while Antarctic krill (like many other polar invertebrates and polar microalgal species) are both stenothermal and very sensitive to temperature change, their growth rates and life history are both microalgae- and temperature-dependent (35). It is possible that thermal effects on diatom distributions and productivity are a contributing factor.

Shifts in microalgal distribution or productivity can also have consequences for biogeochemical cycles, as they are critical for the sequestration of inorganic nutrients (2, 9). Nitrogen fixation (36), carbonate fluxes (14, 37) and the phosphorus, iron, silicate and carbon cycles are dominated by microalgae (2, 38). Biogeochemical processes are similar to food webs in that they are dependent on diatom and other microalgal productivity, grazing and sinking rates. These factors are all directly affected by the morphology, physiology, metabolism and subsequent macromolecular composition of microalgal groups, which in turn, are affected by temperature (39, 40).

Effects of nutritional quality of primary producers

The growth rates and nutritional quality of upper-trophic level consumers are reliant on the nutritional quality of diatoms and other primary producers (41). For example, slower growth rates were evident in juvenile abalone and prawns fed on low-protein microalgal cultures, although oyster growth rates remained unaffected (41-43). In Antarctica, copepods, herbivorous zooplankton and omnivorous consumers such as Antarctic krill, consume microalgae, particularly diatoms (44, 45). These consumers rely, sometimes exclusively on microalgal sources of macromolecules. For example, fatty acid stores of herbivorous zooplankton are sourced primarily from microalgae, with as little as 2 % originating from *de novo* biosynthesis (46). Additionally, diatoms are the primary microalgal source of carbohydrates for marine zooplankton (47). Both temperature variations and extremes can affect microalgal nutritional quality due to compositional changes that occur when resources are directed to compensatory processes (48). If temperature affects macromolecular composition in Antarctic microalgae, consumer growth rates or nutritional content could be affected (10).

Ecological modelling deficiencies

The relevance of understanding the temperature-induced physiological responses and subsequent molecular composition of diatoms far exceeds simple knowledge gathering for this understudied class of organisms. Global modelling experiments, currently being used to predict the effect of climate change on ocean ecosystems, are difficult to place in a biological or ecological context. This is due firstly, to the limited understanding of the physiological performance of phytoplankton and secondly, to the use of a high variety of analytical methods to generate data sets which are highly variable and not easily compared (49). An understanding of species-specific physiological responses to environmental change, particularly for important microalgal groups such as diatoms, is necessary in order to improve these models and predict community-wide shifts as environments change (9, 49).

Effects of temperature on diatoms

Diatoms are ubiquitous unicellular eukaryotes found in all aquatic environments. They are characterised predominantly by their unique silica frustules (50). Diatoms are common to temperate waters but are also well adapted to living in extreme and highly variable environments, such as those imposed by polar seasonality, having acquired many adaptations for thermal resilience (8, 51, 52).

Temperature is an important factor regulating diatom growth and composition (24). Thermal variations have been shown to affect growth rates (17, 53, 54), photophysiology (55-57), metabolism (58) and also protein and lipid composition (28, 59-61) of diatoms and other microalgae.

Effects of temperature on diatoms - macromolecular composition

Thermal variations can result in the allocation of carbon towards storage molecules, usually lipids (62). However, many studies (Table 1) have shown that optimal temperatures correlate with the maximum lipid content in diatoms (17). This was evident in tropical diatoms *Nitzschia closterium*, *Nitzscia paleacea*, *Amphiprora sp*. (17, 63), a temperate diatom *Navicula incerta* (although with narrowly maximum lipid content) and the polar diatom *Navicula glaciei* (17). The effects of temperature on lipid content can be variable in diatoms, however, it has been established that increased saturation of diatom lipids or fatty acids is often associated with increasing temperature, which assists in the maintenance of membrane fluidity (17, 61, 64-66). This has been demonstrated in *Navicula sp*. (28), *P. tricornutum* (64, 66), *Chaetoceros muelleri* (67) and *Odontella aurita* (68).

The relationship between culture temperature and protein content in diatoms is less clear. In a study including six diatoms, protein (and lipid) content did not change linearly with temperature. All species, however, had higher protein levels at the lowest temperature (10 °C) and four diatom species also had increased protein levels above 20 °C (10). High protein levels at low temperature, was explained by the need to increase enzyme content or to maintain membrane fluidity (69). The Antarctic diatom *Navicula glaciei* had lower protein levels at lower growth temperatures (6 °C to 9°C) and higher levels at 14 to 30 °C (28). Additionally, protein levels in the tropical diatom *Chaetoceros* CS256 decreased significantly when culture temperature exceeded 30 °C. This was comparable with earlier studies and was explained by protein denaturation and impairment of enzyme regulators associated with high temperature (53 and references therein).

Effects of temperature on diatoms - photophysiology

Diatoms are photosynthesising organisms and photosynthesis is highly sensitive to temperature (3, 51, 70, 71). Additionally, the enzyme-dependent photosynthetic processes have thermal optima that often differ from thermal optima for growth, further complicating the elucidation of the effects of temperature on these processes (70). Diatom photosynthesis is also the primary (but not exclusive) mediator of survival and both energetic and molecular productivity (3, 72). The effects of temperature on diatom physiology and photophysiology, in particular, are therefore of major concern for this study. Light harvesting efficiency (α), electron transport rate at saturating light ($rETR_{MAX}$) photosynthetic efficiency (F_V/F_M) and growth rates are important physiological measures (73), all of which can be affected differently by temperature.

The light harvesting efficiency is the initial slope of the rapid light curve (74). In eukaryotic microalgae, this measure is generally insensitive to temperature, primarily because photosynthesis at low-light is limited by photochemical processes that are not enzyme-dependent, however, there are exceptions (75). In the benthic diatom *Cylindrotheca closterium* for example, α varied at extreme (5 °C and 35 °C) temperatures (76). In four Arctic sea ice diatoms, α reduced as temperature increased from 5 °C to 15 °C (70). Light harvesting efficiency can be altered by pigment concentrations or by the number or size of light harvesting complexes, comprised of proteins and chlorophyll molecules (70, 77).

The relative electron transport rate at saturating light estimates the maximum photosynthetic capacity which occurs when the photosynthetic rate is limited either by electron transport chain processes or enzyme activity in the Calvin cycle (78, 79). The effect of temperature on electron transport rates seems to vary between taxa. For example, electron transport rates in a diatom community (comprising >95% *Nitzschia stellata*) varied only minimally with temperatures ranging from -6 °C to 6 °C (80). Alternatively, a positive linear relationship between the maximum electron transport rate (ETR_{MAX}) and temperature was demonstrated in the benthic diatom *Cylindrotheca closterium* although the rate reduced dramatically at temperatures above 30 °C (76). Similar results were found in a study involving five benthic diatom species, however as temperatures exceeded 25 °C, $rETR_{MAX}$ varied dramatically between species (57). In contrast, electron transport rate of *T. pseudonana* was stated to be independent of temperature over a 24 °C range (81).

The photosynthetic efficiency or maximum quantum yield (F_V/F_M) is a measure representing the maximum electrons transported per photon of light absorbed. Intraspecific differences in F_V/F_M are the result of photosystem II (PSII) reaction centre damage (26). In the benthic diatom *Cylindrotheca*

closterium F_V/F_M decreased slightly, but significantly, with increasing temperature from 5 °C to 35 °C (76). Similarly, two Antarctic benthic diatoms *Gyrosigma subsalinum* and *Odontella litigiosa* had decreasing ratios of F_V/F_M as temperatures exceeded 4 °C (76). In the sub-arctic pelagic diatom *Pseudo-nitzschia granii*, F_V/F_M was consistent at mid-range temperatures but decreased at the lowest (8 °C) and highest (20 °C) temperatures (26). In short-term experiments a similar pattern was observed; F_V/F_M of *Odontella aurita* remained stable at intermediate temperatures (16 to 28 °C) but reduced significantly at temperatures outside of this range (68).

Effects of temperature on diatoms – growth rates

Diatom growth rates often have a predictable response to temperature increases, whereby photosynthetic activity and growth increase as optimal temperatures are approached, followed by a decrease in photosynthetic activity and growth (8, 64, 68, 70). While the growth rates of polar and temperate diatoms follow this general pattern, polar diatom growth rates gradually reduce as temperature increases, while in temperate diatoms, a small temperature range separates optimal growth rates from lethal thresholds (26 and references therein).

FTIR spectroscopy - a recent advance in algal research

Fourier Transform Infrared (FTIR) spectroscopy is a powerful, non-destructive and rapid technique used to analyse biological material. It can discriminate and determine relative concentrations of microbial cellular macromolecules and, in conjunction with modelling, can be used to classify cells according to a related variable of interest, such as the nutrient status of microalgae (8, 82-85). FTIR is an emerging method in phycological research but remains underutilised. This research aims to demonstrate whether ATR-FTIR in conjunction with Partial Least Squares Regression (PLSR) modelling, can classify diatoms according to their growth temperature. Accordingly, this section describes the history, development and application of FTIR to demonstrate its utility in this arena. Naumann published a comprehensive and historical review on IR (or vibrational) spectroscopy of intact cells in the year 2000, therefore, I will briefly describe the fundamentals and history of IR spectroscopy, as outlined by Naumann and others, but will focus on more recent advances in molecular biology (86).

The infrared (literally 'below red' in reference to its position in the electromagnetic spectrum) spectral region (10 000 cm^{-1} to 10 cm^{-1} wavenumbers) is emitted as thermal radiation. It includes the near-IR (NIR), mid-IR and far infrared (FIR) spectral regions, which are all applicable for spectroscopy. The principal of IR spectroscopy lies in the specificity of IR absorption by molecular functional groups. These functional molecules (e.g $-CH_3$, C=O) have specific vibrational frequencies

dependent on both their atomic composition, structure and orientation (86). In an irradiated sample, wherever wavelength frequency and molecular vibrational frequency correspond (resonant frequencies), that wave or part thereof will be absorbed by that molecule. When a region of the IR spectrum at a known intensity is simultaneously passed through a sample, detection and quantification of the unabsorbed IR waves reveal the molecular composition of the sample (86).

Since its inception in the early 1900s, the potential for IR spectroscopy to differentiate between microbes was realised in the 1950s and 1960s (87, 88). However, it was considered impracticable due to the high initial costs of equipment and the high level of IR absorption by the water content of biological material. These barriers, combined with both computational and spectroscopic limitations at the time, essentially led to a hiatus in IR microbial analysis for the following two decades (86). Other methods for analysing the chemical composition of a sample included separation methods such as gas chromatography-mass spectrometry (GC-MS) and High Precision Liquid Chromatography (HPLC). While these methods are very sensitive and have many applications, they can also be destructive, time-consuming and costly biochemical analytical methods. GC-MS and HPLC methods require the extraction, molecular separation and quantitative chemical analysis of cells, discriminating microbes based on species-specific lipid biological markers for example (89). Nuclear Magnetic Resonance (NMR) is another alternative however, this requires the use of radioactive labelling. While these techniques were (and still are) valuable in many fields requiring quantitative biochemical analysis, their disadvantages created the need for better alternatives more specific to whole-cell biochemical analysis. The need for rapid analysis became especially important as the persistent problem of bacterial resistance required the traceability of microbial relatedness, to both identify bacterial transmission between patients, and to enable appropriate preventative action (83).

IR spectroscopy was a promising non-destructive alternative to these traditional methods, needing both minimal sample preparation and small amounts of biological material while taking approximately two minutes to scan a sample (90). By the 1980s and 1990s, the advantages of FTIR spectroscopy were clear but it was difficult to detect the relatively low energy of atomic interactions sensed by the IR spectrum. The advent of interferometers, however, facilitated beam splitting and recombination, enabling an entire spectral region to pass through a sample simultaneously. This system results in what is called an interferogram, which comprises both constructively and destructively interfering waves, so the IR spectrum of the sample requires Fourier transformation prior to reaching the detector. Subsequently, Fourier back-transformation techniques were applied

to the interferogram, culminating in the IR spectrum recorded for further data analysis (91). This increased both the signal-to-noise ratios and the speed of data acquisition, advancing the position of FTIR spectroscopy in biomedical fields (89, 91, 92).

FTIR spectroscopy was subsequently used in the 1990s to determine the total chemical composition of cells, distinguishing between proteins, membranes and cell walls (92, 93). At the time, 'molecular fingerprints' were compared with known spectral bands to identify particular chemical functional groups or cellular substructures. Computerised searching capabilities were also developed to rapidly and unequivocally differentiate these fingerprints (93). However, these technological improvements introduced further complications. The high-resolution characterisation of complex and heterogenous biological material resulted in the detection of many interfering substances. Additionally, the multivariate nature of spectral comparisons, whereby data consists of thousands of wavenumbers (variables) and measurements (replicates/observations), compounded the accumulation of noisy data (94, 95). These factors drove the need for data analysis methods that alleviated interfering factors and rapidly incorporated massive data sets, to generate meaningful information.

Although technologies at the time had not overcome all of these complications, by 1998 FTIR spectroscopy was used to differentiate between different conformations of lipids and proteins (96). In another study that year, the high-resolution nature of FTIR was confirmed with the demonstrated ability to differentiate single-gene knockout mutants in yeast cells (91, 97).

The advantages of FTIR spectroscopy are highly applicable to microalgal studies. Rapid analysis is imperative for ecologically-based microalgal studies, enabling the necessarily large quantity of measurements required to effectively represent naturally variable populations (9). Additionally, FTIR spectroscopy produces high-quality measurements from relatively low amounts of biological material, which is important when analysing microalgae due to their typically low population densities and small size (85, 98).

Despite these advantages, FTIR spectroscopy was not applied to microalgae until 1999, by Kansiz *et al* (99). Five cyanobacterial strains were analysed throughout several growth phases. FTIR spectroscopy and chemometric methods (the data-based interpretation of chemical information) accurately discriminated between these cyanobacterial strains and correctly separated them from a eukaryotic reference group (99).

Two years later, Giordano *et al*. (2001) compared FTIR with conventional methods for determining the effects of nitrogen limitation in diatoms. This study demonstrated that environmentally induced variations in the relative proportion of macromolecular pools could be characterised rapidly and accurately using FTIR spectroscopy (100). A similar study in the same year also had success in determining the nutrient status of microalgae in response to phosphate limitation. FTIR spectroscopy (and microspectroscopy) was shown to be comparable with conventional methods, effectively and rapidly demonstrating previously reported shifts in carbon allocation towards different macromolecular pools, in response to phosphate-limitation in all four microalgal species studied (101). Beardall *et al*. (2001) concluded that, despite the bulky and expensive spectrometers available at the time, FTIR spectroscopy had considerable potential for the study of algal physiology in response to environmental variation (101). In a separate review by the same author, it was noted that FTIR spectroscopy also had its limitations because macromolecular variations were not specific to limitation or repletion of any one nutrient, with different nutrient-limitations potentially producing the same compositional response in cells (102).

Subsequent studies used combinations of FTIR, Raman microspectroscopy or synchrotron light sources to monitor changes in living cells based on their nutrient status. These studies demonstrated that with increased sensitivity and high signal-to-noise ratios, living cells could potentially be classified based on nutrient limitation (103, 104). Despite the demonstrated potential of FTIR, few studies successfully implemented microbial discrimination or classified nutrient limitation in microalgae, purportedly because insufficiently rigorous classification and discrimination algorithms led to a lack of precision (83, 105).

Heraud *et al*. (2006) used multivariate analysis methods to classify the nutrient status of individual microalgal cells, despite the inherent variability of microalgal response to nutrient limitations. The study tested the effectiveness of chemometric methods and spectral pre-processing techniques, in particular, improving the ability to reliably classify the nutrient status of microalgae (105). This is difficult because variations in spectra can occur as a result of inter and intra-cellular variability, or due to minute differences in irradiation from the laser source. Additionally, spectra can have broad sloping baselines due to fluorescence. Pre-processing methods such as transformation of the spectra diminish these variations to ensure spectra can be effectively compared with each other. To determine the best form of transformation of raw spectra, Heraud *et al*. (2006) applied several different methods including Multiplicative Scatter Correction (MSC), in addition to Extended Multiplicative Scatter Correction (EMSC), (106) and the Standard Normal Variate (SNV)

method (105). Additionally, first and second derivatives were generated to describe band-shifts, peak broadening and intensity changes. PCA was used to simplify the data-sets by grouping spectra based on similarity, firstly to reveal general trends in the dataset and secondly to determine the optimal number of principal components necessary to represent only the chemical differences in samples. Loading plots were assessed to determine important spectral regions (bands) contributing the greatest variance. Heraud *et al*. (2006) found that this was only possible for spectra that had been transformed by the EMSC pre-treatments (105). To test the feasibility of predictive models, spectra from N-replete and N-deplete treatments were randomly split into calibration and validation sets. Two classification approaches were tested on the same calibration set, namely Partial Least Squares (PLS), (107) and Soft Independent Modelling by Class Analogy (SIMCA), (108). It was concluded that, with or without transformation, unambiguous classification using SIMCA was unreliable. PLS using first and second derivates performed well and also benefited from EMSC pre-processing, however, it was clear from the study that different treatments altered the performance of the model. It demonstrated that classification of algal nutrition status was possible, however, the type of transformation should be evaluated by comparing differences in the Root Mean Square Error of Calibration (RMSEC) and the Root Mean Square Error of Validation (RMSEV). This is an objective means of evaluating the best form of pre-treatment, where small and similar error values indicate the best fit (105). This study was expanded upon in a subsequent study by the same author the following year, primarily by increasing the number of spectra taken from individual cells to account for intracellular variability and to improve classification accuracy (82). By this time vibrational spectroscopy was being used to demonstrate either individual, population or intraspecific-level variability, in response to their environment (109, 110).

Additional systems were also used in conjunction with FTIR spectroscopy to improve its application. FTIR spectroscopy is a form of transmission spectroscopy, which requires the suspension of liquid or ground solid samples in a suitable matrix. There are problems associated with these preparative techniques such as the preparation time required and more importantly the risk of highly variable results due to methodological differences (91). Attenuated Total Reflectance (ATR) is an alternative to transmission spectroscopy which avoids the complications associated with transmission spectroscopy. In ATR-FTIR spectroscopy, the IR beam passes through a high-refractive index crystal (e.g. diamond) at an angle exceeding the critical angle required for total internal reflection. A dried sample is placed in contact with the crystal window and is penetrated by an evanescent wave which essentially leaks from the crystal due to the reflectance, before reaching a detector,

thus avoiding the need for IR transmission. This facilitated both reduced preparation times, high reproducibility between samples and high user-to-user precision (91).

Since the evolution of viable chemometric methods, FTIR spectroscopy has a demonstrable track-record, signifying its potential for microalgal research. It has been successfully applied in the fields of microbial ecology, environmental, agricultural and food sciences and in the areas of forensics, medicine and the pharmaceutical industry (8, 9, 85, 98). In microalgal studies, FTIR spectroscopy has already been used to demonstrate both the physiological effect of nutrient deficiency (101, 111, 112), heavy metal contamination (85), temperature and salinity variation (8, 113), and even for identifying the composition of algal fossils (114).

The present study was inspired by a recent proof-of-concept study that used FTIR spectroscopy, validated by mass spectrometry, to predict changes in cellular composition and carbon productivity of an Antarctic diatom in response to salinity and temperature variations. In this novel study, spectroscopy based predictive models were used to quantify the productivity of the Antarctic diatom, *Chaetoceros simplex* under a fully factorial design over a range of temperatures (-1.8 °C, 2 °C and 5 °C) and three salinities (30, 34 and 70). Calibration and validation data sets were compiled for two treatments, consisting of mass spectrometry-derived values (vector of 'Y' variables) representing three parameters: cellular nitrogen levels (a protein proxy), carbon content and ^{13}C uptake (signifying carbon productivity). The corresponding FTIR spectra (matrix of 'X' variables) in the PLSR models are derived from the macromolecular composition of cells in response to temperature and salinity variations. A third treatment (2 °C only) was used as an independent data set, where the three PLSR models (one for each 'Y' component above) predicted the "unknown" nitrogen and carbon content and carbon productivity under the same salinity and temperature regimes. The models predicted carbon productivity with R^2 values between of 0.762 and 0.844, with a prediction root mean square error of 10% to 15% of the maximum 'Y' value, demonstrating that spectra-based models are accurate predictors of cellular response to environmental variation (8).

The aim of the present study was to investigate the impacts of temperature on the growth, photophysiology and macromolecular composition of the Antarctic diatom *Corethron pennatum*. Additionally, this study was intended to assess whether ATR-FTIR spectroscopy and modelling can be used to predict the growth temperature of 'unknown' samples of *C. pennatum*. Specifically, the objectives were:

1. To compare potential differences in macromolecular composition of the Antarctic diatom *Corethron pennatum* cultured at different growth temperatures between 0 °C and 4.5 °C.

2. To compare potential differences in the growth rate and photosynthetic efficiency of *C. pennatum* across this range of temperatures.
3. To determine how accurately ATR-FTIR spectroscopy-based Partial Least Squares Regression (PLSR) models can predict *C. pennatum* growth temperature.

In order to achieve these objectives, I used ATR-FTIR spectroscopy to generate spectral signatures based on the macromolecular composition of the Antarctic diatom C. pennatum grown at 0 °C, 1.5 °C, 3.0 °C and 4.5 °C. Photophysiological parameters were also measured to potentially explain marked differences in macromolecular composition. Specifically, I determined which macromolecules increase or decrease in response to growth temperature and whether photophysiological performance and growth rates of *C. pennatum* varied with temperature. I also determined the R^2 value of the ATR-FTIR spectroscopy-based PLSR predictive models to demonstrate its accuracy.

Methods

Culture conditions

A culture of *C. pennatum* was derived from a single cell following isolation from coastal waters taken during the *RV Investigator* voyage IN2017_V01 from Hobart (Tasmania, Australia) to the Totten Glacier region (Sabrina Coast, East Antarctica). The sample from which this cell was taken (ID: In2017_V01_C45) was collected on the 2nd December 2017 from site four (station CI4: Latitude (S): -64.71233333, Longitude (E): 117.7175, SST: 1 °C). Taxonomic classification was performed on-board the vessel, based on frustule morphology using light microscopy. The diatom was identified as *Corethron pennatum* (Grunow) Ostenfeld (previously *Corethron criophilum* Castracane, *Corethron hispidum* Castracane); a non-filamentous, radially symmetrical centric diatom with articulated hooked spines that extend from the circular valve margin (115, 116). The culture was stored in Antarctic seawater at 2 °C in 50 mL vented bottles. Culture bottles were imported into Australia under Australian Quarantine and Inspection Service (AQIS) permit IP17000156 and transported to Macquarie University PC2 quarantine facility. On the 3rd May 2017, cultures were transferred to a Monash University quarantine facility and stored at 3 °C ±1 °C under the same permit.

Axenic, continuous cultures of *C. pennatum* were maintained in natural seawater collected from Portsea Front Beach, Victoria, Australia, by a commercial supplier. During the early experimentation stage, a routine total metal analysis of Monash University's seawater stocks, conducted by

Australian Laboratory Services Pty Ltd, Scoresby, Victoria, detected higher than normal levels of aluminium, at 0.07 mg L^{-1}. Following investigations, no action was taken in response to these elevated aluminium levels, (as experiments were in progress) due to the following reasons: 1. Elevated aluminium was detected in only one of three tanks, which resulted in a two-third dilution of affected water because water is drawn equally from all tanks as a normal operating procedure. 2. Of the limited studies available, equivalent aluminium levels did not reduce growth rates in either freshwater, brackish or pelagic diatoms. Previous studies demonstrated that aluminium toxicity did not inhibit freshwater diatom growth rates until a threshold of ≥ 24 µmol dm^{-3} Al (equivalent to 647 mg L^{-1}) was met (117). In the freshwater diatom, *Asterionella ralfsii* cell-size, but not growth rates decreased at ≥ 2.8 µmol L^{-1} (equivalent to 75 mg L^{-1}) of aluminium (118). In the benthic diatom, *Navicula salinarum* growth rates increased while in the pelagic diatom, *Thalassiosira weissflogii* growth rates were constant at ≥ 0.10 µmol L^{-1} (equivalent to 2.7 mg L^{-1}) of aluminium (119). Microalgal growth rate is a reliable indicator of fitness; therefore, these levels were considered unlikely to limit *C. pennatum* fitness (24). During routine observations of stock cultures (in affected seawater), no difference was detected in *C. pennatum* cultures nor in triple replicates of 11 other Antarctic diatom species under culture. Every indication suggested that the seawater would not inhibit *C. pennatum* growth. In all cultures, seawater was sterilised by filtration through a Millipore membrane (0.22 µm pore-size) and enriched with f/2 supplements (120).

In microalgal culture mediums, dissolved inorganic carbon (DIC) concentrations are depleted with culture age by photosynthetic microorganisms. Additionally, cell-clumping and settling can occur in stagnant culture mediums, resulting in self-shading (121, 122). Both culture mixing and CO_2 supply were, therefore, maintained via filtered aeration through a sterile glass tube at the bottom of each culture vessel. Culture vessels were kept under axenic conditions which prevented regular pH monitoring. As bubbling rates can influence pH levels, they were reduced to the minimum bubbling required to maintain water circulation (123).

Each culture vessel was illuminated by an inbuilt white light LED array generating continuous incident irradiance at 50 µmol photons m^{-2} s^{-1}. Inoculant culture stocks were also maintained in continuous light at a similar irradiance. This intensity was comparable with recent similar studies (8, 113, 124-126). Many algal studies use 100+ µmol photons m^{-2} s^{-1} (127-129) however 50 µmol photons m^{-2} s^{-1} was chosen to maintain continuity between storage and experimental conditions. Time constraints necessitated the lower light intensity as differences in light conditions between storage and treatments, were likely to induce changes in chlorophyll content,

photosynthetic capacity and photoprotective activation, which needed to be avoided (79). Modification of photosynthetic apparatus can take weeks during acclimation; however, some adjustments can occur in as little as four days (55, 79). I also chose to use continuous light which excluded the possibility of diurnal fluctuations, which can occur during cyclical light exposure (130). This prevented the need to take growth rate measurements at the same time every day, which would be required to avoid any potential cyclical deviations.

C. pennatum was cultured at a salinity of 34 ppm. This was the approximate average salinity recorded during sample collection from Antarctic waters and is consistent with pelagic habitats in that region (113, 131). This salinity also allows my results to be compared with several similar studies conducted at 34 ppm (3, 8, 113). It was also, incidentally the inherent salinity of the seawater obtained for culturing, therefore, salinity adjustments were unnecessary throughout the experimentation process. This was confirmed through continuous monitoring.

Diatoms were cultured in 100 mL glass culture vessels housed in two MC 1000-OD Multi-cultivators (Photon Systems Instruments, Drasov, Czech Republic). Culture vessel locations within the Multi cultivator chambers were placed into a randomly selected position during each inoculation. This was performed as a mandatory experimental practice but was also considered necessary because the chilled water inlet and outlet are positioned at opposite ends of the chamber. The unidirectional water flow could therefore potentially cause a slight temperature gradient along the length of the culturing chamber. Regular monitoring during the experimental period, however, demonstrated highly precise temperature readings throughout the chambers.

Establishment and maintenance of exponential phase

Cultures were maintained and harvested during the mid-exponential phase to avoid nutrient limitations associated with increasing culture age (77, 123, 132). Exponentiality was established during pilot trials conducted from 24th April to 12th May 2018. To determine the exponential phase and growth rates, cell counts were taken daily using an Improved Neubauer Haemocytometer. Initial pilot trials included a *Pseudo-nitzscia sp*. and *Fragilariopsis sp*. which had to be abandoned in the interest of completing the project on time. Initial trials solely monitored growth rates in order to ascertain the inoculation rates required to achieve a final cell count (on day 3) of approximately 10^8 cells mL^{-1} (98). The majority of the time, however, was dedicated to attaining a balance between the maintenance of exponential cultures, which requires culture dilution and attaining sufficient biomass for ATR-FTIR spectroscopy procedures. From the initial trials, average growth rates indicated that an initial inoculation rate of 350,000 cells mL^{-1} was required. However, repeated

attempts to achieve the final desired culture concentrations failed. I attempted to rectify this by increasing the inoculation rate to 400,000 cells mL^{-1} which resulted in lower final cell concentrations than the previous culturing attempts. After several failed attempts it was decided that exponentiality was a priority over attaining biomass, as it is essential for avoiding nutrient-limitation which would alter the macromolecular composition of the cells (77, 123, 132). Observations throughout this stage also led to the realisation that any increase in inoculation volume resulted in a decrease in the volume of fresh medium, which was likely to limit nutrient availability and also likely explained the reduced final culture concentrations observed when applying this method. Subsequent research confirmed this logic and procedure was adjusted accordingly (113).

Following initial trials, the exponential phase was maintained by an approximate 80 % dilution every three days with fresh f/2 enriched seawater, maintained at the corresponding treatment temperature. For each treatment, four culture-vessels were maintained, which consisted of three replicates (n = 3) and one for acclimation to the subsequent temperature increment, which was not accessed during culturing (i.e. cell count samples were not taken) to avoid any potential for contamination (133).

Acclimation

In similar studies to ours, microalgae have been acclimated for one week (112, 134) however eight to ten generations have also been stated as a minimum requirement for acclimation (10, 135). Cultures were acclimated for 12 days as a compromise between achieving the minimum number of generations and reducing exposure of axenic cultures to potential infection during dilution.

Axenicity

All culture vessel equipment was autoclaved at 120 °C for 20 min. Equipment and cultures were processed in a sterile laminar flow cabinet, and flask apertures were sterilised with a Bunsen flame to prevent contamination during culture inoculation. Attempts to maintain axenic conditions during inoculation, in conjunction with the need to maintain culture temperatures, caused considerable difficulties during pilot trials and initial experiments. As mentioned in the previous section, my attempts to inoculate culture vessels to achieve specific cell concentrations, required precise inoculant measurements. At that stage, inoculant volumes were transferred from the culturing flask or vessel to the experimental culture vessel (with the f/2 medium maintained at corresponding temperature) via a 25 mL pipette. This method led to many cultures with either low cell counts or non-exponential growth rates (see Figure S1). Through trial and error, it was suspected that this method was rapidly warming the inoculant volume due to the large surface area of the pipette and

the exposure to the flame-warmed air in the laminar flow. I amended the procedure by simply pouring the inoculant from one vessel to another which was rapid but less accurate and precise. This was rectified by placing a pre-filled culture vessel beside the receiving culture vessel, to indicate the appropriate fill level which worked well.

Growth rates

Microalgal growth rate is a reliable indicator of both fitness and metabolic state and is altered by environmental variability. Growth rates were, therefore, continuously monitored throughout the culturing phase. To account for cell-size differences, which can confound growth rate measurements, growth rates were monitored by continuous optical density as a proxy for biomass and calibrated with manual cell counts (24). Optical density readings were taken every thirty minutes with the Multi-cultivator's inbuilt PIN photo-diode detector with 630 *n*m - 750 *n*m bandpass filters. Real-time optical density was measured across a 27 mm optical path using the 750 *n*m wavelength which is relevant for diatoms (as opposed to the 680 *n*m option) and reduces the potential to bias results if cellular Chl *a* content varies (126, 136). As a non-filamentous diatom, *C. pennatum* was selected as an ideal focal organism for this study, as filaments can complicate cell counting methods.

Optical density readings for generating growth curves were to be calibrated with physical cell counts, however optical density readings failed at all culture temperatures, most likely due to the presence of condensation on external coverings of the multi-cultivator, which interfered with optical density sensor readings.

Growth rate was calculated (Figure 1a) based on the formula

$$\mu = \frac{lnN_2 - lnN_1}{T_2 - T_1} \quad (1)$$

Where N_1 and N_2 denote cellular concentrations (cells mL^{-1}) at time one (T_1) and time two (T_2), respectively.

Temperature was automatically controlled via two refrigerated water-baths and recorded daily. The temperature range for experimental treatments was 0 °C, 1.5 °C, 3.0 °C, 4.5 °C and 5 °C, ±0.5 °C for all temperatures. Typical summer-time sea surface temperatures in Antarctic waters range from between -1.8 °C to 4.5 °C (24, 137). Treatments were intended to exceed this range; however, it was limited, firstly because Multi-cultivator limitations prevented the application of sub-zero temperatures, and secondly because growth rates of the 5 °C replicates could not be maintained at an exponential rate and these cultures eventually failed. Additional attempts to culture at this

temperature were not conducted, as the extra time required was likely to have jeopardised project completion. The 5 °C treatments were therefore excluded from statistical analysis.

Photosynthetic capacity – theory and measurement

The photosynthetic performance of *C. pennatum* was measured just prior to FTIR analysis using chlorophyll *a* fluorescence measured on a pulse amplitude modulated fluorometer (PhytoPAM, Heinz Walz GmbH, Effeltrich, Germany) using the formulae of the equations of Eilers and Peeters (1988, ref 138). This section includes a brief description of the theory behind this measuring technique, as this was required in order to fully understand and interpret results.

Until the last few decades, radio isotope ^{14}C-uptake and oxygen evolution were used to measure photosynthetic efficiency. More recently, chlorophyll *a* fluorescence has superseded these methods, although O_2 gas exchange remains useful for growth measurements. Chlorophyll *a* fluorescence is considered advantageous both in the laboratory and *in situ*, as it is an accurate and rapid technique, that firstly, does not require an enclosed system, and secondly does not require the use of radioactive isotopes, which are best avoided in the field in order to limit pollution (5).

This method utilises the properties of the microalgal photosynthetic apparatus, namely photosystem II (PSII), to deduce the quantum efficiency (product of interest, per photon) of photosynthesis by detecting emitted fluorescence (5). As photons are absorbed by chlorophyll molecules in the antenna, electrons are excited to a higher energy state. Electron de-excitation (return to the ground state), results in energy being released either as heat, fluorescence or photochemical energy. Heat emission effectively dissipates energy from photons that have energy levels greater than that required for photosynthesis. Heat loss also occurs when excessive irradiance induces non-photochemical quenching (NPQ), which protects light-harvesting complexes and photosystems from an excess of damaging reactive oxygen species. This NPQ is quantified as a decrease in F_M' as irradiance increases (139 and references therein, 140). Fluorescence is emitted when the de-excitation energy is unable to be converted to photochemical energy in the reaction centres of the antenna. Therefore, fluorescence increases as photochemical efficiency (e.g. electron transport per photon) decreases. Energy is unable to be converted to photochemical energy when reaction centres are full of electrons (‘closed’) and cannot receive additional energy, or when photosynthetic efficiency is reduced (which might occur under environmental stress or as a consequence of high-light adaptation e.g. low chlorophyll concentrations). Fluorescence emitted per photon (fluorescence yield (F)) is therefore inversely proportional to the photosynthetic yield. By inducing open (dark-adapted), high-efficiency (low-light) and closed (saturating-light) antennal

states, measurements of F are used to deduce photosynthetic yield. 'Open' reaction centres, measured in near dark (F_0), have low levels of electrons passing through them (photosynthesis is not occurring) and therefore have maximum electron carrying capacity; 'closed' reaction centres, measured in high-light have a lower capacity to receive excitation energy as they are full of electrons due to photosynthesis (5). This is the basis of PhytoPAM calculations.

Just prior to cell-fixing, a 3 mL aliquot from each culture was transferred to a quartz cuvette. Contents were continuously stirred and maintained at the corresponding growth temperature within the cuvette holder of the PhytoPAM during a 15-minute dark-adaptation period. The yield of photosystem II, which corresponds to F_V/F_M in dark-adapted samples, was then measured based on the following formula

$$Yield = \frac{F'_m - F}{F'_m} \quad (2)$$

where F_m' is the maximum fluorescence following light acclimation, and F is the steady-state fluorescence in light (141-143). Photosynthetic efficiency (Figure 1b) was compared between treatments using data corresponding to the light intensity most resembling growth conditions (64 µmol photons m^{-2} s^{-1}).

Eighteen incremental irradiances from 0 to 610 µmol photons m^{-2} s^{-1} were used to generate rapid light curves. From the light curves, the Phytopharm automatically calculated the relative electron transport rate (rETR) based on the quantum yield of photosystem II, using the formula

$$\mathrm{rETR} = \mathrm{Yield} \times \mathrm{PAR} \quad (3)$$

where the yield equates to the ratio of photons converted to electrons (measured via fluorescence), PAR is the incident photosynthetically active radiation (light intensity - modulated by the PhytoPAM).

Light harvesting efficiency (α) and relative maximum ETR ($rETR_{MAX}$) were calculated from the light curve. The α is the initial slope of the rapid light curve calculated by the PhytoPAM, which represents the slope of the rapid light curve in the light-limiting region (79). $rETR_{MAX}$ is the rETR at light-saturated (maximum rate) of photosynthesis.

Harvest and sample preparation

C. pennatum cells were fixed with 1 % formalin and left to stand for >10 hours, to comply with biosecurity requirements. The formalin solution was discarded during routine cell washing (described later) performed prior to FTIR analysis. Formalin-fixing has been shown to preserve cell

contents such as lipids and proteins with little effect on infrared spectra, even from cross-linking (144, 145). Later work demonstrated that lipids remain relatively unaffected by formalin, however, a significant decrease in amide I peak intensity can occur in formalin-fixed samples. This was attributed to the cross-linking action of formalin which converts amides from secondary to tertiary proteins. This can cause shifts confined to the amide I band peaks, which can misrepresent actual proteins present in living cells, however, all treatments would be similarly affected (146, 147). It is also possible to assign spectral bands based on changes occurring due to fixation as opposed to the expected absorption bands of functional groups (148).

Cell washing is required to remove elements, especially salts, within the growth media with spectral bands that obscure the biological bands of interest (98, 149). Approximately half of each 80 mL cell suspension was transferred into a 50 mL centrifuge tube, then centrifuged at 3000 rpm for 15 minutes. The supernatant was extracted then the remaining cell suspension was added to the tube before repeating the centrifuge cycle. The supernatant was again extracted, and cells resuspended in 20 mL isotonic 400 mM ammonium formate solution. This was repeated twice, which has been shown to prevent the detection of bands associated with salt crystals (98, 150). Following the final supernatant extraction, the remaining cell concentrate (approximately 1 mL) was transferred to Eppendorf tubes. Centrifuge tubes were rinsed with 700 µL of ammonium formate to collect remaining cells. These cells were also added to the Eppendorf tube. The final suspension was then centrifuged at 13000 rpm for five minutes. The supernatant was again extracted, and the mixed pellet was transferred via pipette onto a glass microscope slide and dried at 65°C in preparation for spectroscopy (98, 151). Slides were stored in a desiccator at room temperature for less than 48 hours prior to FTIR analysis. This time constraint was necessary to avoid excessive sample desiccation which resulted in sample flaking, as cells no longer adhere to the slide.

Dehydration of biological material avoids the presence of water, which is the universal complication associated with IR analysis (148). Water efficiently absorbs infrared at various wavelengths, particularly at both the 3400 cm^{-1} and 1645 cm^{-1}, the latter of which obscures the amide I band (91). Dehydration, however, can result in distortions. IR spectral analysis of dehydrated cells can be used to compare cell composition under different treatments, as long as all cells in the analysis are dehydrated (148).

ATR-FTIR spectroscopy, chemometrics and statistics

High cell densities (with dried cells completely covering the 2 mm diamond window) were analysed by ATR-FTIR spectroscopy, to collect average population data and gain high signal-to-noise

ratios (101). Absorbance spectra were measured at the mid-infrared range (4000 cm^{-1} to 800 cm^{-1}) with a resolution of 4 cm^{-1} with 50 co-added scans for enhanced signal-to-noise ratio, on a Bruker Equinox 55 spectrometer (Bruker Optics Inc., Etlingen, Germany) coupled to an ATR accessory with a diamond window (Golden Gate; Thermo Fisher Scientific, Inc, Waltham, MA, USA) and fitted with a liquid-nitrogen-cooled MCT detector. The diamond window was cleaned with pure isopropanol, and a background scan performed, between samples. ATR correction of co-added spectra was generated via extended ATR correction using OPUS (Bruker) software.

Spectral pre-processing and analysis were performed on OPUS-generated data imported into The Unscrambler®. Derivatisation was performed using the Savitsky-Golay algorithm, using the second derivative with 9-point smoothing to correct broad baseline slopes and separate potentially overlapping or obscured bands in the raw spectra (105). This is necessary because the visualisation of either band ratios, intensities or raw average spectra is insufficient for identifying macromolecular variations between treatments. Derivatisation is commonly applied to raw spectra, which identifies local minima and maxima. In the second derivative spectra, (Figure 2) raw spectral maxima become minima and vice versa (152). As model accuracy is pre-processing dependent, I compared the Extended Multiplicative Scatter Correction (EMSC) and the Standard Normal Variate (SNV) normalisation of spectra which resulted in almost identical Root Mean Square Errors (which equate to deviations from the modelled line of best fit) in subsequent PLSR models. SNV was therefore applied to reduce variations due to heterogenous sample thickness (105).

The exclusion of redundant or unimportant spectral data points (at certain wavenumbers) can improve the strength of predictions when discriminating microbes using FTIR spectroscopy (105). Therefore, the regions 3030 cm^{-1} to 2820 cm^{-1} and 1780 cm^{-1} to 680 cm^{-1} were selected as the major biological bands of interest to be included in the analysis.

Principal components analysis (PCA) was applied to the transformed spectral data to easily identify important information which is not easily visualised due to the multivariate nature of spectra. The important principal components were determined from the loadings plots, which identified the spectral regions accounting for major variations in the data. Scores plot were used to visualise any clustering (105).

PLSR modelling was then performed on mean-centred data using the Non-linear Iterative Partial Least Squares (NIPALS) algorithm. Leave-one-out cross-validation was applied to calibrate the models. Additionally, a stratified-random approach was used to select spectra, forming a calibration set (two-thirds of the data) and independent validation set (one-third of the data) that were

mutually exclusive. Each 'Y' variable was the relevant temperature of the growth culture corresponding to the set of 'X' variables which comprised one spectrum for each respective 'Y' variable. The validation set was used to test the model which compared the calibration set RMSE with the validation set RMSE. Once the model was validated and shown to be robust, the above steps were repeated with the addition of a separate prediction data set (17 spectra), to use the built model to predict the growth temperature of 'unknown' samples, based on their spectra.

Following data pre-processing, 2nd derivative spectra were exported to Microsoft® Excel ® for Office 365 for 'manual' area under the curve calculation of relative macromolecular composition of cells, based on the direct ratio of absorbance and concentration that exists according to the Beer-Lambert Law (113).

Statistical analysis was performed using RStudio (Version 1.0.143 – © 2009 – 2016). Where assumptions were met, comparison of relative macromolecule concentrations and photophysiological measurements were performed using one-way ANOVA with Tukey's multiple comparisons. When tests of normality or homoscedasticity assumptions were not met, a Kruskal-Wallis one-way test was performed in place of ANOVA.

Results

Growth rates and photophysiology

The effects of temperature on *C. pennatum* growth rates did not appear to differ across treatments, except at 5 °C. This treatment could not be sustained over the acclimation period, and then demonstrated rapidly reduced cell numbers which is an indicator of mortality (81). For this reason, the 5 °C treatments were excluded from further analysis. *C. pennatum* demonstrated relatively healthy growth (growth mean = 0.70 div d^{-1} ±SD 0.03) at all experimental temperatures (24). Maximum quantum yields (F_V/F_M), are reduced in the 3.0 °C and 4.5 °C treatments (Figure 1b), with a significant difference observed between the two hottest and the two coldest treatments (ANOVA: $F_{3,8}$ = 12.806, P-value = 0.002, *n* = 3). The $rETR_{MAX}$ (Figure 1c) is highest at the lowest temperatures compared to the two higher temperatures, although the difference is not significant between 1.5 °C and 3 °C (ANOVA: $F_{3,8}$ = 17.128, P-value = 0, *n* = 3). Light utilisation efficiency (α, Figure 1d) at 4.5 °C is significantly different from all other treatments (ANOVA: $F_{3,8}$ = 10.726, P value = 0.003, *n* = 3). Cultures grown at the highest temperature have the lowest light utilisation efficiency, indicating that light capturing capacity of the PSII antenna appears to be reduced at this temperature.

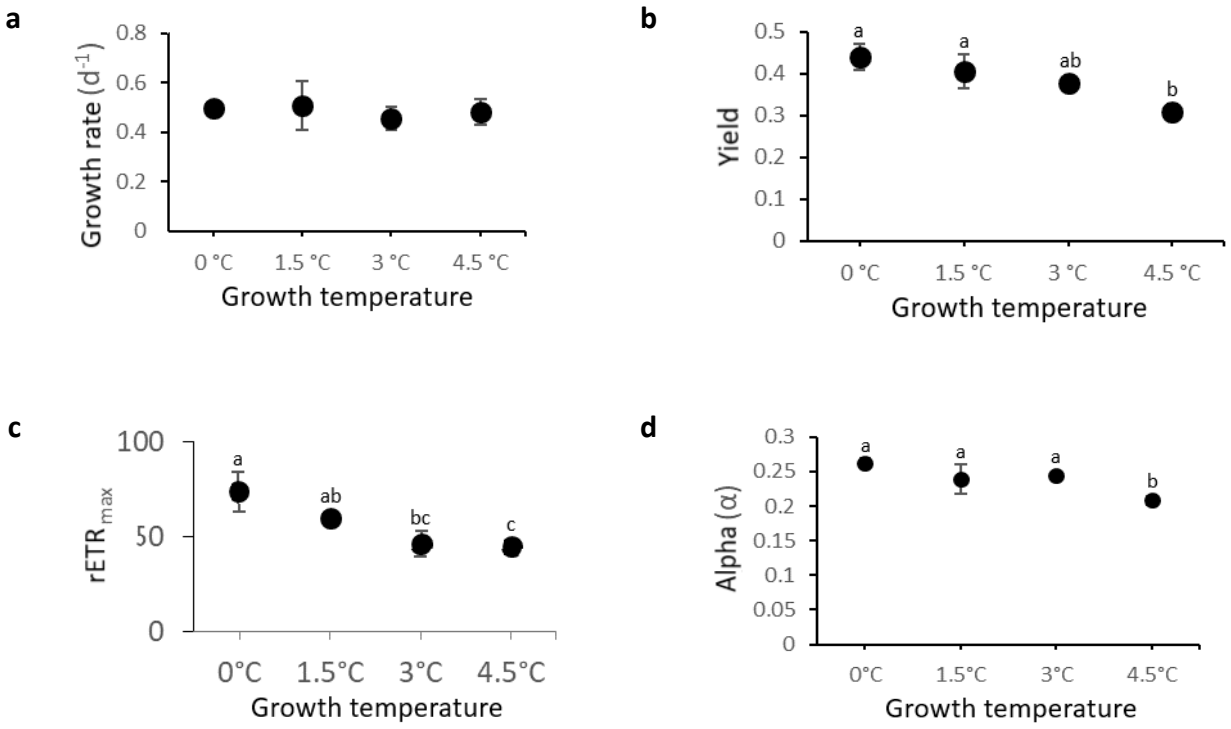

Figure 1. Growth rates (a), photosynthetic efficiency (b), relative electron transport at saturating light (c) and light harvesting efficiency (d) of *Corethron pennatum* cultured at different temperatures. Data represent the mean ± SD (*n* = 3). Significant differences are symbolised by different letters. Growth rates did not significantly vary with growth temperature. A slightly decreasing trend in photosynthetic efficiency (F_V/F_M) which corresponds to yield (b) in dark-adapted samples, is observed, with the 3.0 °C (0.38 SD ±0.01) and 4.5 °C treatment (0.31 SD ±0.02) having lower photosynthetic efficiency compared to both the 1.5 °C (0.41 SD ±0.04) and 0 °C (0.44 SD ±0.03) treatments. The relative electron transport rate in saturating light ($rETR_{MAX}$) is highest at 0 °C (73.57 SD ±10.40) and lower at 3.0 °C (46.20 SD ±3.81) and 4.5 °C (44.60 SD ±1.93). *C. pennatum* also has lower light harvesting efficiency at 4.5 °C (0.21 SD±0.01) compared to all other treatments.

FTIR spectroscopy and macromolecular composition

Spectra with high signal-to-noise ratios were obtained for cells from all treatments. The average second derivative spectrum (Figure 2) revealed noticeable differences in the macromolecular composition of *C. pennatum* between treatments. Diatoms from all treatments have strong and clearly delineated spectral bands associated with the unsaturated fatty acids (UFA), (3014 cm^{-1}), ester carbonyl functional groups from lipids (1740 cm^{-1}), amide I protein bands (~1650 cm^{-1}, ~1630 cm^{-1}) and carbohydrates (1108 cm^{-1} and 1045 cm^{-1}). Variability (see Table S1) appears to be lowest in spectra from the 0 °C treatment. Low variation is also apparent in the 1.5 °C treatment, however, spectra from two biological replicates for this treatment were removed from statistical and data analysis (excluding photophysiology results) due to suspected contamination following harvest. This may explain the low variation observed for this treatment. High variability in absorbance levels between the 3 °C and 4.5 °C is apparent around the carbohydrate (1045 cm^{-1}) and silicate bands (1080 cm^{-1}), which are associated with diatom frustule composition (Kroger08). The absence of peaks around 3400 cm^{-1} and 3250 cm^{-1} (not shown) demonstrate the dehydrated nature of the microalgal cells analysed in this study (85, 148).

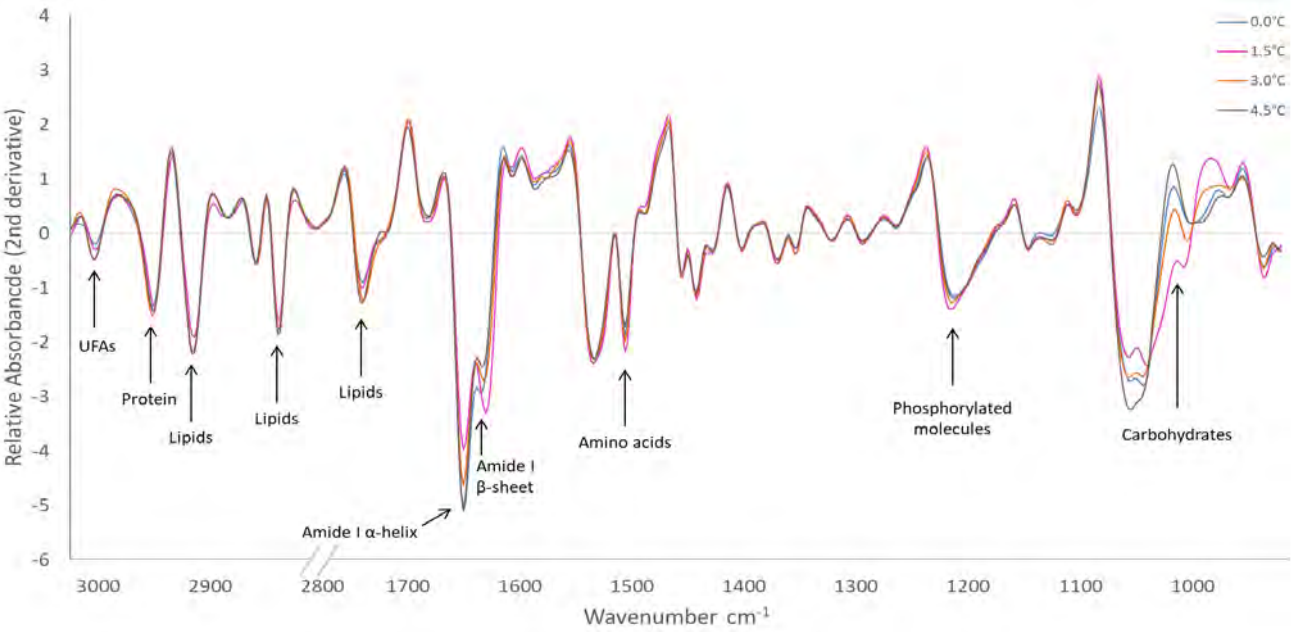

Figure 2. The average second derivative (3030 cm^{-1} to 2820 cm^{-1} and 1780 cm^{-1} to 950 cm^{-1}) of *C. pennatum* spectra. The labels indicate the macromolecules corresponding to the relevant band. The peak at 1743 cm^{-1} corresponds to stretching modes of ester carbonyl (C=O) groups, associated with lipids (148). Two absorption peaks around ~1630 cm^{-1} (β-pleated sheet) and ~1650 cm^{-1} (α-helix) belong to the amide I band and are mainly due to C=O stretching vibrations in peptides (148, 154). The silicate and carbohydrate structure of the diatom frustule explains the high absorbance (at the unlabelled negative peak) around 1080 cm^{-1} (155).

Visualisation of the principal components analysis (PCA) scores plots (Figure 3a) identified a reasonable level of grouping in the data sets. Of the total variance in the data, 78% could be explained by the first two principal components (not shown), however, PC-1 and PC-3 proved to be most important for discriminating between treatments (Figure 3). At PC-1, negatively loaded spectral bands are evident at 1654 cm^{-1} (amide I, α-helix) and 1076 cm^{-1} (Silicate). At PC-3, 1641 cm^{-1} (amide I, α-helix) is negatively loaded. UFAs (3014 cm^{-1}), lipids (1743 cm^{-1}) and amide I β-pleated sheets (1630 cm^{-1}) are all positively loaded at PC-3.

The scores plot demonstrates that with the exception of the 0 °C culture, the higher temperature treatments are increasingly positive for PC-1 (Figure 3a). The 0 °C treatment group is also positive for PC-1. Positive PC-1 scores correspond to high levels of silica and α-helix (especially in the 0 °C and 4.5 °C treatments) and low levels of β-pleated sheets, and carbohydrates (1045 cm^{-1}) as indicated by the intense positive peak (strong minima) visualised in the PC-1 loadings plot. The 1.5 °C treatment clusters with a negative PC-1 score, signifying high β-pleated sheet content compared to other treatment groups and also higher carbohydrate levels corresponding to the 1045 cm^{-1} band. Additionally, the scores plot shows that the 0 °C and 1.5 °C treatment groups are positive for PC-3. These treatments are clearly separated from the negatively scored 4.5 °C treatment group. This demonstrates that lower temperatures have higher carbohydrate (~1066 cm^{-1}) content. The increasingly negative scores of the higher temperature treatments at PC-3 correspond with comparatively high UFA and lipids levels compared to the 0 °C and 1.5 °C treatment groups.

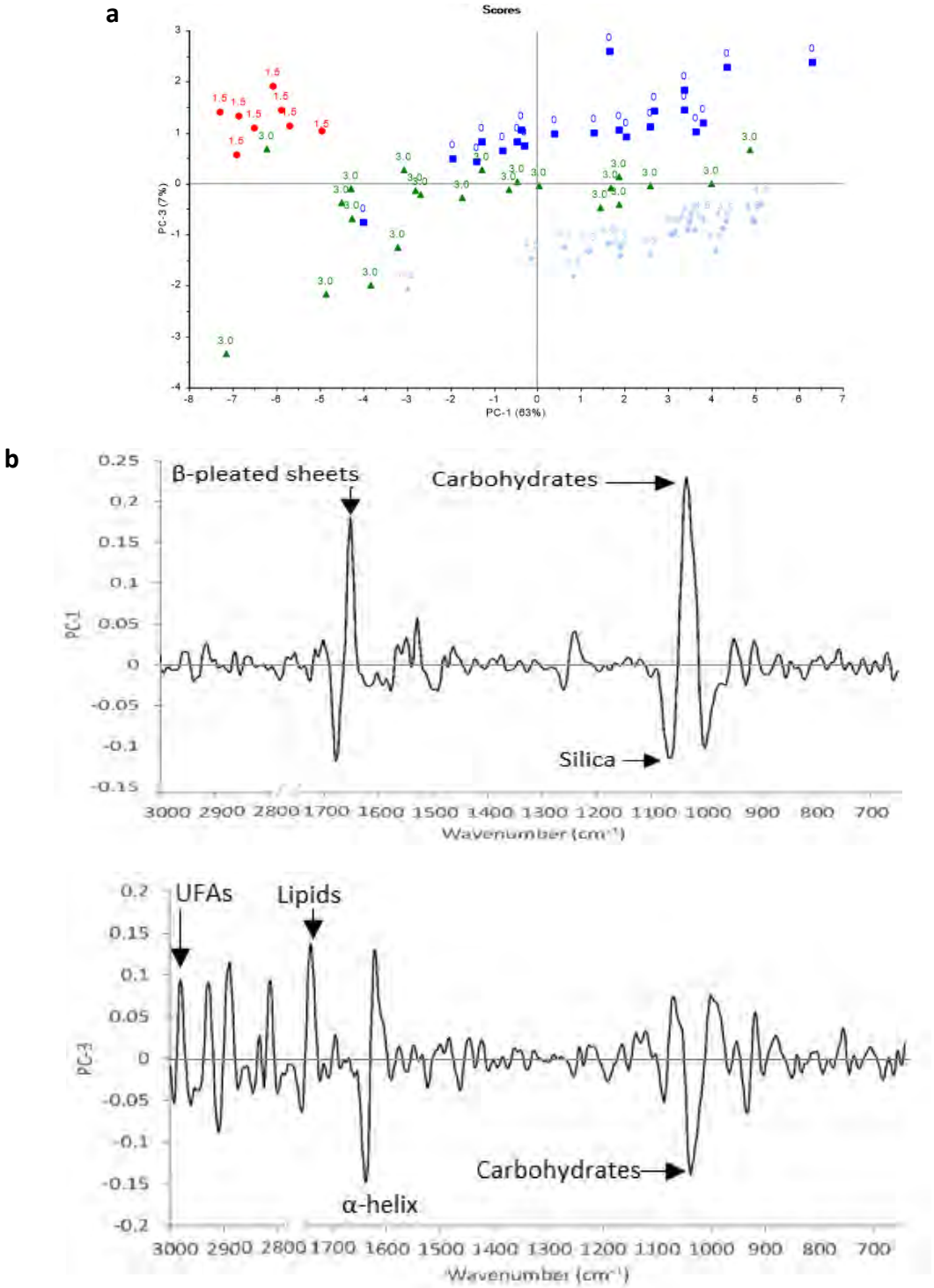

Figure 3. PCA scores plot (a) and loadings plots (b). Principal component one (PC-1) and PC-3 of *C. pennatum*. Spectra from each culture temperature form reasonably clustered groupings. In the loadings plot, negative bands signify an increased absorbance corresponding with positive PC scores. With the exception of the 0 °C culture (which was more negative for PC-2 than the remaining treatment groups (not shown)), an increasingly positive trend is noticeable with increasing growth temperature across PC-1. This signifies that β-pleated sheets and carbohydrates are lower at these higher temperatures. The positive PC-3 scores of 0 °C and 1.5 °C relate to low levels of unsaturated fatty acids and lipids and higher carbohydrate levels. (n = 3 for all treatment groups except the 1.5 °C treatment (n = 1) which had two replicates removed due to contamination following harvest).

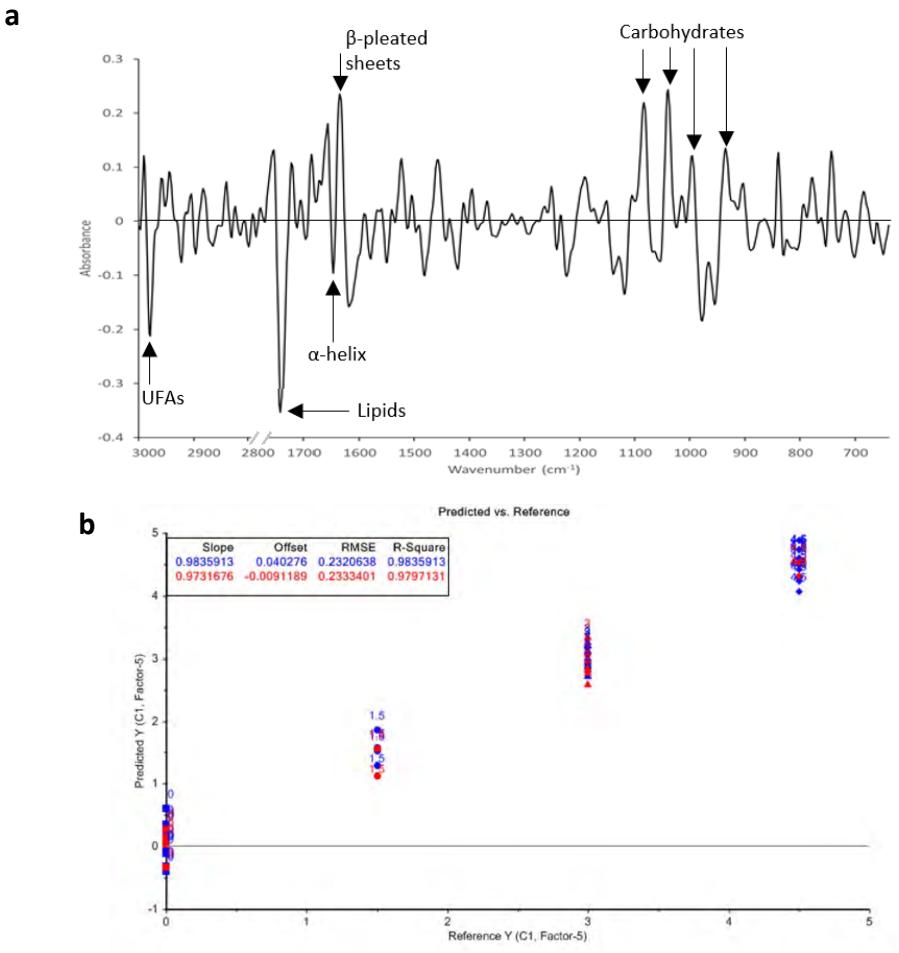

Figure 4. Partial Least Squares Regression model for *C. pennatum* growth temperature. The PLSR five-factor regression vector (a), derived from the normalised 2nd derivative data, represents the string of all regression coefficients (β), multiplied by the corresponding absorbance (χ) values (e.g. $\beta_1\chi_1 + \beta_2\chi_2 + \beta_3\chi_3$ …); essentially, the sum of the resultants gives the predicted temperature. In the predicted versus reference validation plot (b) the linearity is clearly visualised and is supported by the high R^2 and low Root Mean Square Error (RMSE) values in the (blue) calibration (0.98) and (red) validation (0.97) sets.

Leave-one-out PLSR modelling (Figure 4) was performed to discriminate between growth temperatures. The predicted versus reference plot (Figure 4b) demonstrates a high level of predictive accuracy as evidenced by both excellent linearity, Pearson R^2 values close to one and a Root Mean Square Error (RMSE) for both calibration and validations sets, of 0.23. This indicates that the FTIR spectra-based model can predict the growth temperature of *C. pennatum* cells to within ±0.23 °C.

Differences in macromolecular composition between treatments were estimated using the average area under the curve of individual second derivative spectra at biological bands of interest. It was

not possible however, to quantify carbohydrate concentrations in this manner, due to the close proximity and strong influence of nearby silicate bands (Figure 3b). The results (Figure 5a) confirm that unsaturated fatty acid (UFA) content increases with increasing temperature, except at 4.5 °C which is not significantly different from 3.0 °C (one-way ANOVA, $F_{3,69}$ = 187.33, p-value = 0). The greatest difference in UFA levels is evident between the 1.5 °C and 3 °C treatments. The neutral lipids (predominantly triacylglycerols) associated with 1740 cm^{-1} band (85, 156, 157) also vary with temperature (Figure 5b). At 0 °C and 1.5 °C growth temperatures, *C. pennatum* has a lower lipid content (Kruskal-Wallis chi-squared = 52.668, df = 3, p-value = 0) than those cultured at higher temperatures. There is a slight general trend of decreasing protein concentrations with increasing temperature. Protein levels were significantly different (one-way ANOVA, $F_{3,69}$ = 23.87, p-value = 0) but not between all treatments. Protein levels are highest in *C. pennatum* grown at 0 °C and are significantly different from all other treatments; cells grown at 1.5 °C also have a higher protein content than those grown at 4.5 °C (figure 5c). The major observable effect of temperature on *C. pennatum* protein is in the differential ratios of α-helix to β-pleated sheets (Figure 5d) between treatments; α-helix concentrations are lowest and β-pleated sheets levels are highest in the 1.5 °C treatment, compared to cells at all other temperatures. The 0 °C, 3 °C and 4.5 °C have low levels of β-pleated sheets compared to α-helix protein conformations.

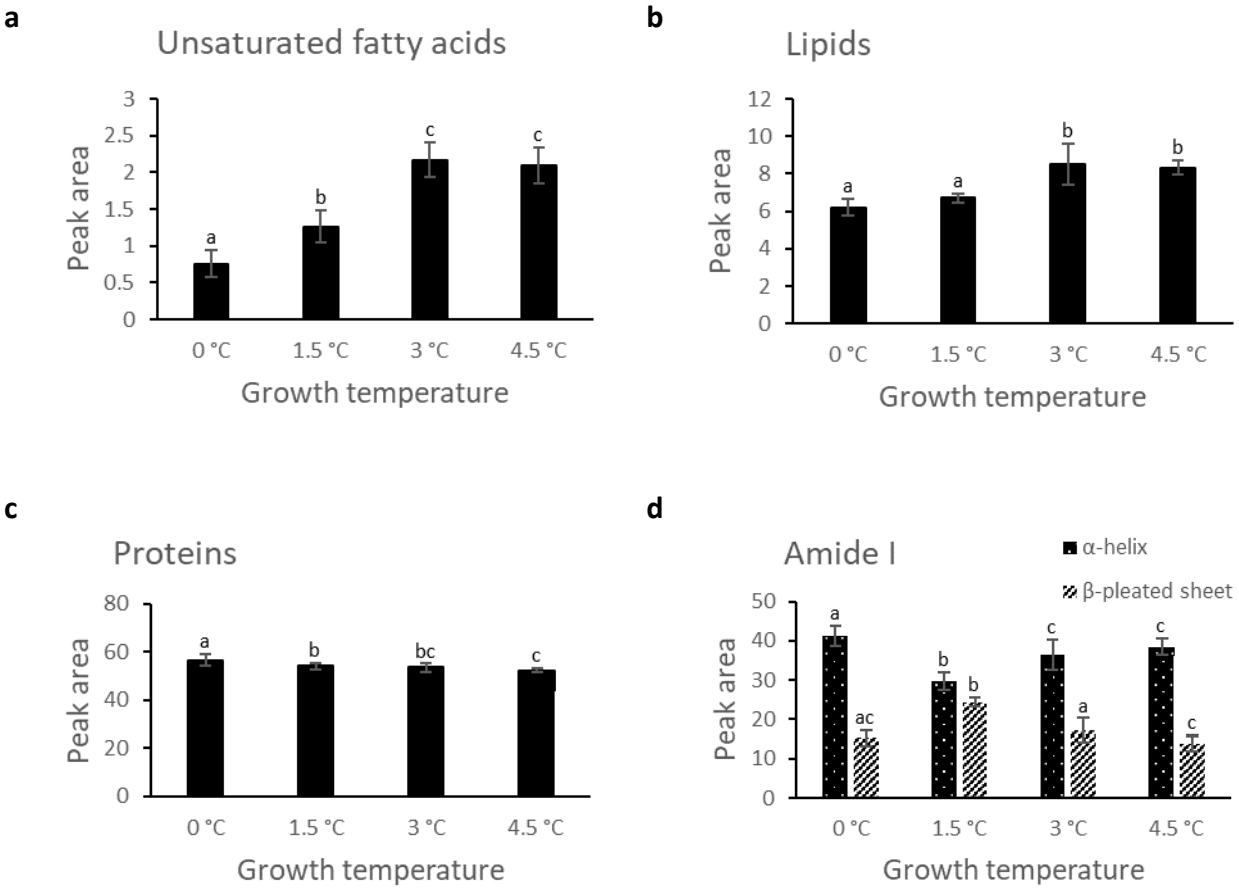

Figure 5. Relative cellular macromolecular concentrations of *C. pennatum*. The concentration of macromolecules derived from the average area under the curve of each infrared spectrum, based on the direct relationship that exists between absorbance and concentration according to the Beer-Lambert Law. Significant differences are symbolised by different letters. *C. pennatum* unsaturated fatty acid (a) and lipid (b) concentrations are greatest at higher temperatures; the relative content of unsaturated fatty acids in the 4.5 °C treatment is 2.09 SD ±0.24 compared to 0.76 SD ±0.24 in the 0.0 °C treatment group. There is a general (but insignificant) trend of slightly decreasing protein concentration (c) in *C. pennatum* as growth temperatures increase; 0 °C cultures, however, have higher protein content (56.57 SD ±2.34) than the other treatment groups. The α-helix and β-pleated sheet levels (d) are similar in the 1.5 °C treatment (29.83 SD±2.21 and 24.37 SD ±2.21 respectively). The remaining treatments have higher levels of α-helix than β-pleated sheets with the highest level (41.30 SD ±2.61) present in the 0.0 °C treatment group. Error bars indicate the standard deviation.

Table 1 Overview of diatom response to temperature variations

Species	Light level	Temp (°C)	$T_{opt\ \mu}$ (°C)	μ_{max} d^{-1}	$T_{lipid\ max}$ (°C)	$T_{protein\ max}$ (°C)	$T_{tolerance}$ (°C)	Response	Reference
Amphiprora UMACC 239	42	13 to 38	28	0.25	23 & 28		13 to 33		Teoh et al., 2013
Chaetoceros calcitrans	220	10 to 25	25*	>3*	20*	20*	10 to 25	↑ T = ↑ Growth rate	Thompson et al., 1992
Chaetoceros cf. wighamii	530	20 to 30	20		25	20		↑ T = ↓ Carbohydrates	de Castro Araújo and Garcia, 2005
Chaetoceros CS256	80	25 to 35	27 to 30	0.87	25	27 to 30		↑ T = ↓ proteins	Renaud et al., 2002
Chaetoceros gracilis	220	10 to 25	20*	>1.5*			10 to 25	Growth increased from 10 to 20 °C	Thompson et al., 1992
Chaetoceros gracilis		10 to 25						↑ T = ↓ lipids	Thompson et al., 1992
Chaetoceros simplex	220	10 to 25	25*	>2*	10*	10*	10 to 25	↑ T = ↑ Growth rate	Thompson et al., 1992
Chaetoceros simplex		10 to 25						↑ T = ↓ lipids, ↓ proteins	Thompson et al., 1992
Haslea ostrearia		20, 30						↑ T = ↑ Fatty acid saturation	Dodson et al., 2014
Navicula glaciei	42	4 to 33	4	0.34	4, ~20	14	4 to 30	↑ T = ↓ Growth rate, ↓ PUFA	Teoh et al., 2004
Navicula incerta	42	4 to 32	11	0.38	11*		4 to 32	↑ T = ↓ lipids, ↓ PUFAs	Teoh et al., 2013
Nitzschia closterium	80	10 to 35	20 to 25	0.38	20			↑ T = ↓ lipids	Renaud et al., 1995
Nitzscia paleacea	80	10 to 35	15	0.38				↑T = ↓ lipids. ↑ FA saturation	Renaud et al., 1995
Odontella aurita	300	8 to 24						↓T = ↓ growth rate; ↑ PUFA, ↓ SFAs	Pasquet et al., 2014
Phaeodactylum tricornutum		20, 30						↑ T = ↑ lipids	Dodson and Leblond, 2015
Phaeodactylum tricornutum		20, 30						↑ T = ↑ Fatty acid saturation	Dodson et al., 2014
Phaeodactylum tricornutum		10 to 25						↓T = ↑ growth rates, ↓T = ↑ PUFAs	Jiang and Gao, 2004
Phaeodactylum tricornutum	220	10 to 25	25*	>1.5*	25*	10*, 25*	10 to 25	↑ T = ↑ Growth rate	Thompson et al., 1992
Thalassiosira antarctica	39	-2 to 3						↓ T = ↓ proteins ↓ productivity, stable lipid levels	Tillmann et al., 1989
Thalassiosira pseudonana	220	10 to 25	25*	>2*	10*, 25*	25*	10 to 25	↑ T = ↑ Growth rate	Thompson et al., 1992

T = temperature; OPT μ = optimal growth; PUFA = Poly unsaturated fatty acid; SFA = saturated fatty acid

* estimated, not explicitly stated in study; Light units = μmol photons m-2 s-1

Discussion

To determine the effects of temperature variations on the Antarctic diatom *C. pennatum*, this study used ATR-FTIR spectroscopy, and pulse amplitude modulated fluorometry to determine variations in both physiology and macromolecular composition. Additionally, I generated spectroscopy-based Partial Least Squares Regression (PLSR) predictive models, indicating the relationship between diatom physiology and temperature.

Growth rates

The consistent growth rates of *C. pennatum* across the 0 °C to 4.5 °C temperature range, indicate that the general metabolic state of cells did not vary with temperature (24). Additionally, the healthy growth rates observed at 0 °C indicate that the critical minimum temperature may not have been attained in this study (49, 81). The average growth rates attained (Figure 1a) were almost double that of *C. pennatum* (as *C. criophilum* Castracane) determined in an earlier study (0.21 div d^{-1}) at comparable light intensities and temperatures (24). This was unexpected given that maximum quantum yields (F_V/F_M) ranged between 0.3 (at 4.5 °C) to 0.47 (at 0 °C) in my study. Maximum quantum yield is an ideal indicator of photosynthetic health, averaging around 0.6 to 0.65 in microalgae. Yields below these levels indicate that photosynthetic capacity is reduced due to stress (142, 158). The comparatively healthy growth rates observed, do not suggest that *C. pennatum* cultures were stressed. Cultures in the earlier study appeared not to be aerated, which may explain the differences in growth rate compared with this study, as aeration avoids cell-shading due to settling and ensures a constant CO_2 supply (121, 122). Alternatively, the low quantum yields obtained in this study may have been be due to a methodological error. The background fluorescence (i.e. fluorescence of filtered media) was not set as the base fluorescence prior to analysis. This can result in lower than actual estimations of the maximum quantum yield. However, a fresh media sample was tested for background fluorescence, and was found to be negligible. This explanation, therefore, seems unlikely, but is possible. An additional, alternative explanation for the low maximum quantum yields may be that the irradiance level during cultivation was damaging to PSII. However, *C. pennatum* was cultivated between 50 and 220 µmol photons m^{-2} s^{-1} in the similar experiment mentioned above, and the lowest growth rates were attained at the lowest irradiance level (24). As growth rates and maximum quantum yield are both indicators of microalgal health, it is unlikely that 50 µmol photons m^{-2} s^{-1} is damaging to the photosynthetic apparatus of *C. pennatum* (142, 158).

The evidence provided here suggests that *C. pennatum* is most likely an obligatory psychrophile, considering the inability to maintain cultures at 5 °C for the duration of the acclimation period and the eventual failure of all cultures at this temperature. However, it should be noted that 5 °C may not be the lethal threshold of *C. pennatum*. Despite the axenic culture conditions, all *C. pennatum* cultures grown at 5 °C had high bacterial loads prior to culture failure. Therefore, there is a possibility that 5 °C is the optimal temperature for bacterial fitness in this case, as opposed to a lethal threshold of *C. pennatum*. It is my conclusion however, that 5 °C is the lethal threshold for *C. pennatum*, because results agree with an earlier study, where optimal growth temperature of *C. pennatum* (named *C. criophilum* Castracane) was between 3 °C and 5 ° ±1 °C, with a lethal threshold of 6 °C ±1 °C, which aligns well with the present study (24). This supports the hypothesis that Antarctic diatoms are obligatory psychrophiles, which has also been indicated by several studies (24, 159). There are exceptions, however. The Antarctic diatom *Navicula glaciei*, for instance, survived temperatures ranging from 4 °C to 30 °C (28).

The lethal thermal threshold of organisms is an important factor influencing community structure (160). Additionally, the thermal optimum and thermal range of microalgae are closely linked to their biogeographical boundary, while interspecies variance also determines succession during seasonal shifts (11, 113). It has been proposed that organisms capable of physiologically adapting to high temperatures, will be dominant as a result of global warming (160). In a recent study, the polar diatom *Chaetoceros simplex* was cultured at -1.8 °C, 2 °C and 5 °C. Both maximum growth rates and maximum protein, carbon and energy content were achieved at the highest temperature, in conditions comparable to my study. *Chaetoceros simplex* have high phenotypic plasticity, coping well with Antarctic meltwater, pelagic and sea ice conditions (8). *C. pennatum* however, are more restricted to open waters in Spring (161). My results suggest that ideal conditions for *Chaetoceros simplex* survival and growth (5 °C) are potentially lethal to *C. pennatum*, and both these species inhabit Antarctic pelagic environments, demonstrating the potential for assemblage shifts as sea surface temperatures increase. Others suggest, however, that Antarctic microalgal assemblages will be determined by ice formation and decay, as opposed to physiological plasticity of individual species (162).

Photophysiology

Although strictly photochemical processes such as light absorption, reaction centre energy transfer and reaction centre charge separation are temperature-independent, light harvesting efficiency (α) is considered insensitive to temperature but can vary (5, 26, 75, 80). Light harvesting efficiency did

appear to be affected by growth temperature in *C. pennatum* at the highest temperature (4.5 °C) suggesting that pigment or light-harvesting complexes are affected by temperature in this species (70, 77). This suggests that the photophysiological performance of *C. pennatum* is inhibited by increasing temperature.

In some diatoms, $rETR_{MAX}$ increases as temperature increases, while minimal changes occur in other diatom species (76, 80). It does, however, appear that once a maximum thermal threshold is met, electron transport rates decrease in many diatoms studied (57, 76, 80). In *C. pennatum*, $rETR_{MAX}$ was higher at 0 °C and 1.5 °C and lower at and 4.5 °C suggesting that this temperature is close to the maximum thermal threshold for *C. pennatum*.

A decrease in $rETR_{MAX}$ with no change in α implies either impairment or regulation of the light-independent reactions of photosynthesis (i.e. the Calvin cycle) as opposed to an effect on the rates of light harvesting (78, 101). Across the 0 °C to 3 °C gradient, consistent α values were observed; a decreasing trend in $rETR_{MAX}$, however, was observed as temperature increased from 0 °C to 3 °C. This suggests that $rETR_{MAX}$ was limited by temperature-dependent downstream processes (101). Additionally, α did decrease at 4.5 °C which could indicate a decrease in either the number or pigment content, of light harvesting complexes at this temperature (70, 77). It is, therefore, possible that either downstream regulatory processes or an impairment in the light-harvesting apparatus are responsible for the reduction in light harvesting efficiency observed between 0 °C and 3.0 °C. However, impairment of the light-harvesting apparatus is likely at 4.5 °C, with an associated reduction in the photosynthetic capacity of *C. pennatum*.

In diatoms, PSII maximum quantum yield (photosynthetic efficiency; F_V/F_M) can decrease as temperature increases or as temperatures exceed an upper or lower optimal level (26, 76). In *C. pennatum* F_V/F_M was significantly different between the 0 °C to 3 °C range but decreased at 4.5 °C which was similarly observed in the Antarctic diatoms *Gyrosigma subsalinum* and *Odontella litigiosa* (76). These decreases suggest that these higher growth temperatures result in PSII reaction centre damage in *C. pennatum* which can impede photophysiological performance.

Macromolecular composition - lipids & fatty acids

The major macromolecular products of diatom photosynthesis are carbohydrates (chrysolaminarin) and lipids (67). Additionally, relatively high rates of polysaccharide catabolism occur in both light and dark periods, suggesting that carbohydrates assume the role of food in diatoms, while lipids are reserved to withstand extreme environmental conditions, assisting long-term survival (163-165). Maximal microalgal lipid concentrations have, however, been reported to occur at optimal growth

temperatures (17, 28, 59, 63). This trend is evident in many diatoms including tropical, temperate and polar species where excess photosynthetic products are stored as neutral lipids, predominantly triacylglycerols (67, 166, 167). My results showed an opposite correlation (Figure 3b) between lipid content and carbohydrate content, in addition to higher lipid levels observed in *C. pennatum* grown at 3 °C and 4.5 °C. High lipid levels should indicate that 3 °C and 4.5 °C are optimal growth temperatures for *C. pennatum*, however, a concomitant increase in growth rates was not evident. Additionally, photosynthetic rates were lowest at the higher temperatures, suggesting that temperatures exceeding 1.5 °C are, stressful for *C. pennatum* (142, 158).

It seems that fatty acid saturation in *C. pennatum* however, is in contrast with most diatoms, including polar species. Fatty acid saturation tends to decrease with colder temperatures to maintain membrane fluidity (63, 123, 168). This is particularly important for polar species as microalgal growth at near-freezing temperatures depends on the capacity to synthesise polyunsaturated fatty acids and other cold-adaptive molecules (123, 169, 170). *C. pennatum* has lower concentrations of unsaturated fatty acids at the lowest growth temperatures (0 °C and 1.5 °C) which contrasts with every study encountered during this research (Table 1, refs 17, 63-65, 68). For example, high polyunsaturated fatty acid levels are present at low temperatures in the polar diatoms *Fragilariopsis curta*, *Navicula gelida* var. *antarctica*, *Nitzschia medioconstricta*, and *Navicula glaciei* (28, 168). Additionally, the temperate or tropical diatoms (Table 1) *Phaeodactylum tricornutum*, *Odontella aurita*, *Navicula incerta, Haslea ostrearia* and *Nitzscia paleacea* all had higher degrees of saturation with increasing growth temperature which is necessary for membrane stability at higher temperatures (17, 63, 65, 68, 123, 171).

While fatty acid saturation in many microalgae follow this general pattern, it has also been stated that any relationship between growth temperature and saturation is likely to be species-specific (53 and references therein, 64). My results suggest this may be true, however, closer inspection of one study involving the diatoms *Nitzscia paleacea* and *Nitzschia closterium* revealed that neither diatom demonstrated a consistent positive linear correlation between fatty acid saturation levels across a 10 °C to 30 °C temperature range. Additionally, they had higher monounsaturated and polyunsaturated fatty acid concentrations respectively, within a 5 °C temperature increment in both cases, which is the range used in the current study (63). It is therefore possible, or even likely, that the limited temperature range used in my study is not indicative of a positive trend at temperatures outside of this range. Further to this, photosynthetic efficiency is impacted by the thylakoid membrane's lipid composition and degree of fatty acid

saturation (169, 172). In photosynthetic organisms, higher levels of unsaturated fatty acids stabilise or aid the assembly of photosynthetic membrane proteins such as light harvesting complexes (LHCs) and photosystems, particularly at low temperatures (173, 174). The apparent opposite correlation between unsaturated fatty acid levels and photosynthetic efficiency in *C. pennatum* contrasts with this strategy and therefore deserves further investigation.

Macromolecular composition - Proteins

The effect of temperature on protein synthesis appears to be species-specific, although, in diatoms, high protein levels have been associated with temperature extremes, as a likely mechanism for maintaining either biochemical reactions or membrane fluidity. In contrast, protein denaturation can occur at very high temperatures (10, 53, 123). Thomas *et al*. (1992), suggested that microalgae minimise protein content at their optimal growth temperature (10). This is not true for all diatoms, however. For example, the polar diatom *Chaetoceros simplex* grown between -1.8 °C and 5 °C, achieved both maximum growth rates, and protein levels at the same (highest) temperature (8). In contrast, the protein content of the Antarctic diatom *Navicula sp*. was lowest at the lowest growth temperature tested (4 °C), which was also its optimal growth temperature (28). *C. pennatum* protein concentrations were highest at 0 °C with a small but significant decrease between the 0 °C and 4.5 °C treatments. Considering the increased photosynthetic rate demonstrated by *C. pennatum* at the lowest growth temperature, which is an indicator of microalgal health, it is unlikely that *C. pennatum* has minimum protein levels corresponding with optimal growth temperature, as suggested by Thomas *et al*. (1992). Additionally, *C. pennatum* contrasts with the Antarctic *Navicula sp*. mentioned above, although protein levels in the *Navicula sp*. may differ at 0 °C.

Protein concentrations can mediate photosynthetic rates in microalgae. In saturating light, carbon fixation is hypothesised to be the rate-limiting processes in photosynthesis (70, 175), which involves (not exclusively) Rubisco-dependent processes (Ribulose-1,5-bisphosphate carboxylase/oxygenase) in the chloroplast (70, 175). The protein-heavy Rubisco enzyme present in the chloroplasts of temperate, tropical and polar microalgae, (and all plants) catalyses the carboxylation or oxygenation of ribulose-1,5-bisphosphate in the Calvin cycle and is exceedingly temperature-dependent (175, 176). Additionally, the minimum affinity coefficient of Rubisco occurs between 3 °C and 5 °C (175). Higher concentrations of Rubisco have been noted in Antarctic microalgal strains, compared to mesophilic strains, possibly as a compensation for the reduced activity of Rubisco at low temperatures (176). However, only a few examples of this adaptation exist, supposedly because it is energetically inefficient (174). Rubisco is essential for the Calvin cycle and dominated by

β- pleated sheets (177). If Rubisco levels increased at lower temperatures in *C. pennatum*, high levels of β-pleated sheets would be expected in the 0 °C and 1.5 °C (113). However, only the 1.5 °C culture has increased levels of β-pleated sheets, compared to both warmer and cooler treatments. Results of this study, therefore, suggest that *C. pennatum* is unlikely to increase Rubisco content as a low temperature acclimation strategy and other low-temperature adaptations may explain its ability to withstand near-freezing temperatures. This may be important for understanding how increasing temperatures may affect this diatom.

A recently proposed alternative explanation for the success of psychrophilic organisms suggests that increased ATP levels occur at near-freezing temperatures while the reverse is true for mesophilic and thermophilic species. As temperature increases, metabolic rates increase, and energy demands are higher as a consequence. Thermophilic and mesophilic organisms increase ATP production to satisfy this demand and growth rates increase as a consequence (178). In contrast, psychrophiles have been found to increase ATP levels as temperatures decrease, yet growth rates do not increase as a result (178). Additionally, the low temperatures experienced by polar diatoms limit the rate of carbon fixation (70, 175, 179). The reduced rate of energy consumption by carbon fixation must be balanced by a reduced supply of electrons, which is not limited in saturating light (179). Photosynthetic organisms can accomplish this by adjusting the photochemical efficiency of PSII (via altered pH gradients), subsequently reducing electron transport rates to downstream processes (180). In *C. pennatum* however, $rETR_{MAX}$ was highest at 0 °C and growth rates were not significantly different under all temperature treatments suggesting, firstly that electron supply is not reduced at low temperature and secondly that growth rates did not increase with increasing electron supply. It is, therefore, possible that *C. pennatum*, like other psychrophiles, diverts excess electrons to ATP synthesis (via PSII cyclic electron transport) at near freezing temperatures to maintain biochemical activity (178). The results of this experiment are insufficient to support this argument for three main reasons. Firstly, high levels of ATP are required to biosynthesise proteins (compared to lipids), and secondly, biomass may have increased. Both of these factors could account for electron consumption (181). Thirdly, an absolute ETRmax would be required in order to support this argument, which was not measured in this study. There is, however, sufficient evidence to recommend further investigation.

Primary productivity, food webs and biogeochemical cycles

Primary productivity is predicted to increase as sea surface temperatures increase (13). *C. pennatum* growth and photosynthetic rates did not increase with temperature, and photosynthetic efficiency

decreased at 4.5 °C. This would suggest that *C. pennatum* productivity could decrease with increasing temperature. However, biomass is a critical parameter for characterising primary productivity (75, 182). My findings may not represent the capacity for *C. pennatum* to accumulate biomass, because, for example, the relationship between photosynthetic efficiency and carbon assimilation is species-specific and therefore cannot be assumed to decrease when photosynthetic capacity is reduced (75). Additional factors include microalgal cell volume, which is often positively correlated with temperature (124, 182) and zooplankton grazing is another factor affecting primary productivity (182). Cell volumes and subsequent biomass were not measurable in this study, firstly because the observed non-symmetric nature of *C. pennatum* frustules at different growth stages rendered cell-morphology measurements almost meaningless and secondly, because there was insufficient biomass available for analysis, due to the limited culture volume (90 mL maximum) of the Multi-cultivators culturing vessels.

Although the results of this study do not necessarily reflect the effect of temperature on the potential for primary productivity, they do demonstrate that peak photosynthetic rates of *C. pennatum* occurred at the lowest temperature. This aligns well with a study based along the southern boundary of the Antarctic Circumpolar Current, where primary productivity peaks were observed at -0.54 °C SD ±0.09 °C and krill distributions peaked at around -0.01 °C ±1.00 °C. Sightings of seabirds and baleen whales, the major predators of Antarctic krill, also correlated well with these peak krill numbers (183). In a separate study, vertical net hauls showed that *C. pennatum* was one of two dominant diatom species in this region (184 and personal comments therein). Sea ice dynamics, polar currents and associated nutrient enrichment, play a major role in these close associations, however, the similar temperature association between the observed high photosynthetic rates in *C. pennatum* and both the peak primary productivity and upper-level consumer numbers in the Southern Ocean could be correlative, or it could suggest that sea surface temperature can influence these food web dynamics. This deserves further attention and highlights the importance of ecological modelling in predicting the potential effects of climate change on these interconnected communities.

Thermally induced shifts in macromolecular composition translate to changes in the nutritional value of diatoms, which can have flow-on effects for marine food webs. Lipids for example, are high energy molecules that serve as vital energy sources for Antarctic zooplankton (170, 185). Lipid levels in *C. pennatum* were elevated at the highest temperatures, which would appear to be advantageous to microalgal consumers, however, these benefits may be outweighed firstly by the concomitant

drop in the equally vital carbohydrate levels, which was evident in this study (47). Secondly, lipid accumulation is often oppositely correlated with microalgal biomass, which is an important element in primary productivity (165).

The growth of upper-trophic level consumers in the Southern Ocean is primarily reliant on microalgal sources of protein and grazer-growth rates can decrease if protein sources are limited (41-43, 186). As apex consumers, humans could also experience altered diets if microalgal macromolecular composition is affected by increasing temperature, as essential fatty acids and proteins are often sourced via fish consumption (39). The decreasing levels of protein evident in *C. pennatum* as temperatures increase, warrants further investigation into the effects of temperature on microalgal composition.

Variations in primary producer nutritional values can affect some microalgivore species, while others are unaffected (41-43, 46). The variations in macromolecular composition observed with temperature increases in this and other microalgal studies (Table 1), could therefore differentially affect the growth rates and survival of competing consumers (41). Changes in microalgal composition could therefore result in assemblage shifts throughout Southern Ocean food webs.

Alternatively, thermally induced compositional changes in Antarctic diatoms or other microalgae could modify zooplankton behaviour, with subsequent knock-on effects impacting the food web. As an example, ingestion rates can vary dependent on microalgal attributes; immature Antarctic krill fed a choice of two differently sized microalgae, moderated ingestion rates according to the respective microalgal lipid content (187). This suggests that changes in microalgal nutritional value could affect nutrient and energy transfer efficiency to upper-level consumers, potentially altering both food web structure and biogeochemical cycles (188, 189). In understanding these processes, however, evolutionary ecology needs to be considered. For example, herbivorous zooplankton can adapt to shifts in lipid availability. Additionally, if the observed increases in lipid-levels with increasing temperatures occur in other microalgae, this may include an increase in the synthesis of toxic lipids by primary producers. The subsequent anti-predatory effects may further modify community dynamics (39).

There is the possibility, however, that thermally-induced changes in microalgal composition may be inadvertently counteracted by other environmental effects of temperature. For example, the reduced protein levels observed in (the pelagic) *C. pennatum* as temperatures increased, may be concomitant with increased protein levels in sea-ice diatoms, which has been shown to occur when sea-ice duration and extent is reduced by prolonged warmer temperatures (113).

The consistent growth rates across the temperature range used in this study suggest that the effect of temperature on *C. pennatum* may not affect biogeochemical cycles. Growth rates, however, do not necessarily represent biogeochemical performance as inputs may vary despite a steady growth rate (81).

ATR-FTIR spectroscopy

While cultured organism-based predictive models may not be considered biologically relevant, the high predictive capacity demonstrated by spectroscopy-based modelling in this study demonstrates that this technique or variations of it can be highly valuable for predicting microalgal response to climate change. Current primary productivity models require improved methods for quantifying and describing the microalgal physiological responses affecting marine food webs. Two important questions that need to be resolved to improve these models are, what are the abiotic limiting factors? Which interacting environmental factors have the greatest influence on microalgal physiology? (190). The success of this study demonstrates that ATR-FTIR spectroscopy-based modelling could be used to address the first question. Additionally, recent research has successfully applied very similar methods to demonstrate the abiotic interactions and the physiological response of Antarctic diatoms (8, 113). The success of these studies demonstrates the utility of addressing these questions using ATR-FTIR spectroscopy based predictive modelling. Further to this, techniques such as the portable Raman acoustic levitation spectroscopic system could be applied in the field to characterise the *in vivo* macromolecular composition of individual cells. The non-destructive nature of this method means cells could be analysed then isolated for culturing and subsequent ATR-FTIR spectroscopy analysis, providing a field relevant snapshot of cell physiology prior to assessing the effect of abiotic factors on laboratory-grown cultures (104).

Study competencies and limitations / future direction

The trade-off between organismal functional traits (those that affect performance and subsequent fitness), fundamentally govern a species niche and ecological function (191). While this study has demonstrated the effects of temperature on parameters such as photophysiology, growth rates and macromolecular composition in *C. pennatum*, it is also necessary to determine the interactions and trade-offs between these traits to fully understand the broader implications of increasing temperature on primary productivity (81, 191). Considering the importance of both food webs and fisheries, microalgal ecology is increasingly being applied to understand the effects of environmental change (192). The multi-trait approach to temperature-based studies is potentially the way forward, and ATR-FTIR is very promising as a cost-effective, label-free and non-destructive tool which will be invaluable in this domain. Other authors have previously stated the need to

incorporate multiple functional traits and multiple environmental factors into ecological research, which I agree, is warranted (81). For example, the results of this study demonstrate changes in the concentration and structure of both proteins and lipids as temperature increases, however, subsequent levels of energy and nutrient transfer to upper tiers of the food web remain unknown. The dynamics of total cellular composition and environmental perturbance is perhaps too complex to adopt the reductionist approach as individual traits may respond similarly to different environmental perturbations. Photoinhibition, for example, can vary in response to both high light or high temperature, so it is necessary to measure the response of a suite of functional traits in response to multiple environmental stressors, to determine organism performance in response to climate change (81). Additionally, multiple oceanic factors, such as CO_2 concentration, pH and both nutrient and light availability are likely to be altered (in terms of means or variability) and interact as the global climate changes (21, 81). Teasing apart the multiple stressors influencing both taxon-specific and microalgal function will be paramount to understanding the effect of climate change on food webs, fisheries and biogeochemical cycles. However, there remains a need to isolate organism response to individual environmental stressors, such as temperature, to determine whether organism response is due to the stressor or to the interaction of multiple stressors, highlighting the need to retain both approaches.

Species-specific studies may also provide a limited understanding of the effects of temperature increases on biochemical cycles. For example, frustule silicification is (not exclusively) dependent on growth rate and affects whole cell density (193, 194). Dense silicification of cells may provide defence against predation or alternatively, could result in rapid sinking (194). Subsequently, vertical carbon export (sinking) could increase as a result, affecting biogeochemical cycles. In both cases, nutrients and energy are removed from the immediate food chain, rendering protein and lipid variations unimportant at this level. Understanding the interactions between morphological and physiological traits is therefore necessary for understanding the effect of temperature on food webs and biogeochemical cycles (81). Behavioural traits too, deserve attention. Whilst diatoms dominate polar regions and have a significant role in oceanic elemental cycling there are many other contributors. Similar studies investigating the taxon-specific responses of microalgal groups are required, to better characterise the relationship between oceanic temperature variations, food web dynamics and biogeochemical cycles (81).

It is also necessary to ensure that ecological functions are fully characterised, to provide context for ecology studies and modelling. For example, mixotrophy is common in microalgae and

heterotrophic strategies increase with rising temperature, with a concomitant reduction in electron transport rates. If this is widespread, it is likely to have significant effects on both net primary productivity and global carbon sequestration (195). This might be especially important if, like *C. pennatum*, mixotrophic microalgae have reduced electron transport rates as temperature minimally increase. Thermal responses are, however, often either taxon- or species-specific, further demonstrating why species-specific data remains relevant (26).

Previous studies have shown that, in order to understand the effects of temperature on growth and physiology, results need to be placed in context. For example, one study found that growth rates of eight different microalgal species increased with rising temperatures, however, 25 °C was the highest temperature applied, and no decline in growth was detected at this temperature (10). The optimal and lethal thermal thresholds have not been established and so it is difficult to place results in context. This study is similar in that minimum thermal thresholds were unable to be attained as sub-freezing temperatures could not be applied to the Multi-cultivators. An improvement to this study in order to more effectively contribute to ecological models would be to increase the temperature range applied, to gain biologically and geographically relevant information (26). Additionally, this study effectively excluded genotypic variation (by culturing a clone) to obtain environmental, (not genetic) variations, however genotypic variation is also important. For example, different thermal optimums and critical minimum temperatures were associated with several strains of the same species, using a similar approach to this study, whereby cultures were grown under a range of temperatures in otherwise identical conditions (49). The single isolate of *Corethron pennatum* used in this study is insufficient for representing the species.

Conclusion

It is evident from this research that 4.5 °C negatively affects the photosynthetic capacity of *C. pennatum*. At higher growth temperatures, *C. pennatum* has reduced photosynthetic rates, higher lipid and unsaturated fatty acid levels and lower protein and carbohydrate levels. This indicates that increasing sea surface temperatures may be beneficial to microalgal grazers, providing greater levels of high-energy lipids and essential unsaturated fatty acids to upper trophic tiers. However, this comes at a cost to protein and carbohydrate levels, which are also vital to microalgal grazers. Any benefit provided by increasing sea surface temperatures is significantly outweighed by the high risk of exceeding the lethal threshold of diatoms such as *C. pennatum*, particularly in polar regions where some diatoms have a narrow thermal-window for survival (24, 71, 196).

The knowledge gained through this research can potentially contribute to global modelling experiments, helping to predict the effect of climate change on Southern Ocean ecosystems (9, 49). Additionally, this research has demonstrated that ATR-FTIR spectroscopy and spectra-based predictive models can accurately classify diatoms according to their growth temperature, based on variations in macromolecular composition. The high level of precision and accuracy of this technique would make it invaluable for ecophysiological research, potentially avoiding the inter-laboratory variability currently hindering ecological modelling efforts (91).

References

1. Field CB, Behrenfeld MJ, Randerson JT, Falkowski P. Primary production of the biosphere: integrating terrestrial and oceanic components. *Science* 1998; **281**: 237-240.
2. Sarthou G, Timmermans KR, Blain S, Tréguer P. Growth physiology and fate of diatoms in the ocean: a review. *Journal of Sea Research* 2005; **53**: 25-42.
3. Petrou K, Doblin M, Ralph P. Heterogeneity in the photoprotective capacity of three Antarctic diatoms during short-term changes in salinity and temperature. *Marine Biology* 2011; **158**: 1029-1041.
4. John J. *A beginner's guide to diatoms*. Liechtenstein: A. R. G. Gantner Verlag; 2012.
5. Beer S, Björk M, Beardall J. *Photosynthesis in the marine environment*. Björk M, Beardall J, editors. Ames, Iowa: Wiley Blackwell; 2014.
6. Arrigo KR, Worthen DL, Lizotte MP, Dixon P, Dieckmann G. Primary production in Antarctic sea ice. *Science* 1997; **276**: 394-397.
7. Finkel Z, Matheson K, Regan K, Irwin A. Genotypic and phenotypic variation in diatom silicification under paleo-oceanographic conditions. *Geobiology* 2010; **8**: 433-445.
8. Sackett O, Petrou K, Reedy B, Hill R, Doblin M, Beardall J, et al. Snapshot prediction of carbon productivity, carbon and protein content in a Southern Ocean diatom using FTIR spectroscopy. *International Society for Microbial Ecology* 2016; **10**: 416-426.
9. Murdock J, Wetzel D. FT-IR Microspectroscopy Enhances Biological and Ecological Analysis of Algae. *Applied Spectroscopy Reviews* 2009; **40**.
10. Thompson PA, Guo Mx, Harrison PJ. Effects of variation in temperature. I. On the biochemical composition of eight species of marine phytoplankton. *Journal of Phycology* 1992; **28**: 481-488.
11. Boyd PW, Strzepek R, Fu F, Hutchins DA. Environmental control of open-ocean phytoplankton groups: Now and in the future. *Limnology and oceanography* 2010; **55**: 1353-1376.
12. Gille ST. Warming of the Southern Ocean since the 1950s. *Science* 2002; **295**: 1275.
13. Boyd PW, Doney SC, Strzepek R, Dusenberry J, Lindsay K, Fung I. Climate-mediated changes to mixed-layer properties in the Southern Ocean: assessing the phytoplankton response. *Biogeosciences* 2008; **5**: 847-864.
14. Smetacek V. Diatoms and the Ocean Carbon Cycle. *Protist* 1999; **150**: 25-32.
15. Bergstrom DM, Convey P, Huiskes AHL. *Trends in Antarctic terrestrial and limnetic ecosystems: Antarctica as a global indicator*. Dordrecht: Springer; 2007.
16. Clarke A, Murphy EJ, Meredith MP, King JC, Peck LS, Barnes DK, et al. Climate change and the marine ecosystem of the western Antarctic Peninsula. *Philosophical Transactions of the Royal Society of London B: Biological Sciences* 2007; **362**: 149-166.
17. Teoh M-L, Phang S-M, Chu W-L. Response of Antarctic, temperate, and tropical microalgae to temperature stress. *Journal of Applied Phycology* 2013; **25**: 285-297.
18. Meredith MP, King JC. Rapid climate change in the ocean west of the Antarctic Peninsula during the second half of the 20th century. *Geophysical Research Letters* 2005; **32**.
19. Boyd PW, Doney SC. The impact of climate change and feedback processes on the ocean carbon cycle. Ocean biogeochemistry: Springer; 2003, pp 157-193.
20. Thomas MK, Kremer CT, Klausmeier CA, Litchman E. A global pattern of thermal adaptation in marine phytoplankton. *Science* 2012; **338**: 1085-1088.

21. Boyd PW, Lennartz ST, Glover DM, Doney SC. Biological ramifications of climate-change-mediated oceanic multi-stressors. *Nature Climate Change* 2015; **5**: 71.
22. Kobiyama A, Tanaka S, Kaneko Y, Lim P-T, Ogata T. Temperature tolerance and expression of heat shock protein 70 in the toxic dinoflagellate Alexandrium tamarense (Dinophyceae). *Harmful Algae* 2010; **9**: 180-185.
23. Eppley RW. Temperature and phytoplankton growth in the sea. *Fishery Bulletin* 1972; **70**: 1063-1085.
24. Fiala M, Oriol L. Light-temperature interactions on the growth of Antarctic diatoms. *Polar Biology* 1990; **10**: 629-636.
25. Suzuki Y, Takahashi M. Growth responses of several diatom species isolated from various environments to temperature. *Journal of Phycology* 1995; **31**: 880-888.
26. El-Sabaawi R, Harrison PJ. Interactive effects of irradiance and temperature on the photosynthetic physiology of the pennate diatom pseudo-nitzschia granii (bacillariophyceae) from the northeast subarctic pacific. *Journal of Phycology* 2006; **42**: 778-785.
27. Beardall J, Raven JA. The potential effects of global climate change on microalgal photosynthesis, growth and ecology. *Phycologia* 2004; **43**: 26-40.
28. Teoh M-L, Chu W-L, Marchant H, Phang S-M. Influence of culture temperature on the growth, biochemical composition and fatty acid profiles of six Antarctic microalgae. *Journal of Applied Phycology* 2004; **16**: 421-430.
29. Li Y, Qin JG. Comparison of growth and lipid content in three Botryococcus braunii strains. *Journal of Applied Phycology* 2005; **17**: 551-556.
30. de Boer MK, Koolmees EM, Vrieling EG, Breeman AM, van Rijssel M. Temperature responses of three Fibrocapsa japonica strains (Raphidophyceae) from different climate regions. *Journal of Plankton Research* 2005; **27**: 47-60.
31. Montes-Hugo M, Doney SC, Ducklow HW, Fraser W, Martinson D, Stammerjohn SE, et al. Recent changes in phytoplankton communities associated with rapid regional climate change along the western Antarctic Peninsula. *Science* 2009; **323**: 1470-1473.
32. Atkinson A, Siegel V, Pakhomov E, Rothery P. Long-term decline in krill stock and increase in salps within the Southern Ocean. *Nature* 2004; **432**: 100.
33. Cox MJ, Candy S, de la Mare WK, Nicol S, Kawaguchi S, Gales N. No evidence for a decline in the density of Antarctic krill Euphausia superba Dana, 1850, in the Southwest Atlantic sector between 1976 and 2016. *Journal of Crustacean Biology* 2018: 1-6.
34. Moline MA, Claustre H, Frazer TK, Schofield O, Vernet M. Alteration of the food web along the Antarctic Peninsula in response to a regional warming trend. *Global Change Biology* 2004; **10**: 1973-1980.
35. Clarke A. Seasonality in the Antarctic marine environment. *Comparative Biochemistry and Physiology Part B: Comparative Biochemistry* 1988; **90**: 461-473.
36. Falkowski PG. Evolution of the nitrogen cycle and its influence on the biological sequestration of CO2 in the ocean. *Nature* 1997; **387**: 272.
37. Schiebel R. Planktic foraminiferal sedimentation and the marine calcite budget. *Global Biogeochemical Cycles* 2002; **16**: **13**-**1**1-**13**-21.
38. Quere CL, Harrison SP, Colin Prentice I, Buitenhuis ET, Aumont O, Bopp L, et al. Ecosystem dynamics based on plankton functional types for global ocean biogeochemistry models. *Global Change Biology* 2005; **11**: 2016-2040.
39. Arts MT, Brett MT, Kainz MJ. *Lipids in aquatic ecosystems*. Dordrecht, New York: Springer; 2009.
40. Borowitzka MA, Beardall J, Raven JA. *The Physiology of Microalgae*. Borowitzka MA, editor. Cham, Switzerland: Springer International Publishing; 2016.
41. Daume S, Long BM, Crouch P. Changes in amino acid content of an algal feed species (Navicula sp.) and their effect on growth and survival of juvenile abalone (Haliotis rubra). *Journal of Applied Phycology* 2003; **15**: 201-207.
42. Enright C, Newkirk G, Craigie J, Castell J. Growth of juvenile Ostrea edulis L. fed Chaetoceros gracilis Schütt of varied chemical composition. *Journal of Experimental Marine Biology and Ecology* 1986; **96**: 15-26.
43. D'Souza FM, Kelly GJ. Effects of a diet of a nitrogen-limited alga (Tetraselmis suecica) on growth, survival and biochemical composition of tiger prawn (Penaeus semisulcatus) larvae. *Aquaculture* 2000; **181**: 311-329.

44. Laws RM. The Ecology of the Southern Ocean: The Antarctic ecosystem, based on krill, appears to be moving toward a new balance of species in its recovery from the inroads of whaling. *American Scientist* 1985; **73**: 26-40.
45. Flores H, Atkinson A, Kawaguchi S, Krafft BA, Milinevsky G, Nicol S, et al. Impact of climate change on Antarctic krill. *Marine ecology progress series* 2012; **458**: 1-19.
46. Arts MT. Ecophysiology of lipids in pelagic crustacean zooplankton communities. In: Cooksey KE, editor. Molecular Approaches to the Study of the Ocean. London: Chapman and Hall; 1998, pp 329-341.
47. Seckbach J, Kociolek P. *The diatom world*. Seckbach J, Kociolek JP, editors. Dordrecht, London, New York: Springer; 2011.
48. Geider RJ, Osborne BA. Respiration and microalgal growth: a review of the quantitative relationship between dark respiration and growth. *New Phytologist* 1989; **112**: 327-341.
49. Boyd PW, Rynearson TA, Armstrong EA, Fu F, Hayashi K, Hu Z, et al. Marine phytoplankton temperature versus growth responses from polar to tropical waters–outcome of a scientific community-wide study. *PLoS ONE* 2013; **8**: e63091.
50. Armbrust EV. The life of diatoms in the world's oceans. *Nature* 2009; **459**: 185.
51. Ralph PJ, Ryan KG, Martin A, Fenton G. Melting out of sea ice causes greater photosynthetic stress in algae than freezing in. *Journal of Phycology* 2007; **43**: 948-956.
52. Petrou K, Ralph P. Photosynthesis and net primary productivity in three Antarctic diatoms: possible significance for their distribution in the Antarctic marine ecosystem. *Marine ecology progress series* 2011; **437**: 27-40.
53. Renaud SM, Thinh L-V, Lambrinidis G, Parry DL. Effect of temperature on growth, chemical composition and fatty acid composition of tropical Australian microalgae grown in batch cultures. *Aquaculture* 2002; **211**: 195-214.
54. Sandnes J, Källqvist T, Wenner D, Gislerød HR. Combined influence of light and temperature on growth rates of Nannochloropsis oceanica: linking cellular responses to large-scale biomass production. *Journal of Applied Phycology* 2005; **17**: 515-525.
55. Anning T, Harris G, Geider RJ. Thermal acclimation in the marine diatom Chaetoceros calcitrans (Bacillariophyceae). *European Journal of Phycology* 2001; **36**: 233-241.
56. Gao K, Li P, Watanabe T, Walter Helbling E. Combined effects of ultraviolet radiation and temperature on morphology, photosynthesis, and dna of arthrospira (spirulina) platensis (cyanophyta). *Journal of Phycology* 2008; **44**: 777-786.
57. Yun MS, Lee SH, Chung IK. Photosynthetic activity of benthic diatoms in response to different temperatures. *Journal of Applied Phycology* 2010; **22**: 559-562.
58. Rajadurai M, Poornima EH, Narasimhan SV, Rao VNR, Venugopalan VP. Phytoplankton growth under temperature stress: Laboratory studies using two diatoms from a tropical coastal power station site. *Journal of Thermal Biology* 2005; **30**: 299-305.
59. de Castro Araújo S, Garcia VMT. Growth and biochemical composition of the diatom Chaetoceros cf. wighamii brightwell under different temperature, salinity and carbon dioxide levels. I. Protein, carbohydrates and lipids. *Aquaculture* 2005; **246**: 405-412.
60. Hu H, Li H, Xu X. Alternative cold response modes in Chlorella (Chlorophyta, Trebouxiophyceae) from Antarctica. *Phycologia* 2008; **47**: 28-34.
61. Converti A, Casazza AA, Ortiz EY, Perego P, Del Borghi M. Effect of temperature and nitrogen concentration on the growth and lipid content of Nannochloropsis oculata and Chlorella vulgaris for biodiesel production. *Chemical Engineering and Processing: Process Intensification* 2009; **48**: 1146-1151.
62. Sayanova O, Mimouni V, Ulmann L, Morant-Manceau A, Pasquet V, Schoefs B, et al. Modulation of lipid biosynthesis by stress in diatoms. *Philosophical Transactions of the Royal Society B: Biological Sciences* 2017; **372**.
63. Renaud S, Zhou H, Parry D, Thinh L-V, Woo K. Effect of temperature on the growth, total lipid content and fatty acid composition of recently isolated tropical microalgae Isochrysis sp., Nitzschia closterium, Nitzschia paleacea, and commercial species Isochrysis sp. (clone T. ISO). *Journal of Applied Phycology* 1995; **7**: 595-602.
64. Jiang H, Gao K. Effects of lowering temperature during culture on the production of polyunsaturated fatty acids in the marine diatom Phaeodactylum tricornutum (Bacillariophyceae). *Journal of Phycology* 2004; **40**: 651-654.

65. Dodson V, Mouget J-L, Dahmen J, Leblond J. The long and short of it: temperature-dependent modifications of fatty acid chain length and unsaturation in the galactolipid profiles of the diatoms Haslea ostrearia and Phaeodactylum tricornutum. *The International Journal of Aquatic Sciences* 2014; **727**: 95-107.
66. Dodson VJ, Leblond JD. Now you see it, now you don't: differences in hydrocarbon production in the diatom Phaeodactylum tricornutum due to growth temperature. *Journal of Applied Phycology* 2015; **27**: 1463-1472.
67. Chen YC. The biomass and total lipid content and composition of twelve species of marine diatoms cultured under various environments. *Food Chemistry* 2012; **131**: 211-219.
68. Pasquet V, Ulmann L, Mimouni V, Guihéneuf F, Jacquette B, Morant-Manceau A, et al. Fatty acids profile and temperature in the cultured marine diatom Odontella aurita. *Journal of Applied Phycology* 2014; **26**: 2265-2271.
69. DeNicola DM. Periphyton responses to temperature at different ecological levels. *Algal ecology: freshwater benthic ecosystems* 1996: 149-181.
70. Davison IR. Environmental effects on algal photosynthesis: temperature. *Journal of Phycology* 1991; **27**: 2-8.
71. Mock T, Hoch N. Long-Term Temperature Acclimation of Photosynthesis in Steady-State Cultures of the Polar Diatom Fragilariopsis cylindrus. *Photosynthesis Research* 2005; **85**: 307-317.
72. Kirchman DL. *Processes in microbial ecology*. Oxford University P, editor. Oxford: Oxford : Oxford University Press; 2012.
73. Beardall J, Ihnken S, Quigg A. Gross and net primary production: closing the gap between concepts and measurements. *Aquatic Microbial Ecology* 2009; **56**: 113-122.
74. Wong CY, Teoh ML, Phang SM, Lim PE, Beardall J. Interactive effects of temperature and UV radiation on photosynthesis of Chlorella strains from polar, temperate and tropical environments: differential impacts on damage and repair. *PLoS ONE* 2015; **10**: e0139469.
75. Hancke K, Hancke TB, Olsen LM, Johnsen G, Glud RN. Temperature effects on microalgal photosynthesis-light responses measured by o2 production, pulse-amplitude-modulated fluorescence, and 14c assimilation. *Journal of Phycology* 2008; **44**: 501-514.
76. Morris EP, Kromkamp JC. Influence of temperature on the relationship between oxygen-and fluorescence-based estimates of photosynthetic parameters in a marine benthic diatom (Cylindrotheca closterium). *European Journal of Phycology* 2003; **38**: 133-142.
77. Dao LHT, Beardall J. Effects of lead on growth, photosynthetic characteristics and production of reactive oxygen species of two freshwater green algae. *Chemosphere* 2016; **147**: 420-429.
78. Behrenfeld MJ, Prasil O, Babin M, Bruyant F. In search of a physiological basis for covariations in light-limited and light-saturated photosynthesis. *Journal of Phycology* 2004; **40**: 4-25.
79. Ralph PJ, Gademann R. Rapid light curves: A powerful tool to assess photosynthetic activity. *Aquatic Botany* 2005; **82**: 222-237.
80. Arrigo KR, Sullivan CW. The influence of salinity and temperature covariation on the photophysiological characteristics of antarctic sea ice microalgae. *Journal of Phycology* 1992; **28**: 746-756.
81. Baker KG, Robinson CM, Radford DT, McInnes AS, Evenhuis C, Doblin MA. Thermal Performance Curves of Functional Traits Aid Understanding of Thermally Induced Changes in Diatom-Mediated Biogeochemical Fluxes. *Frontiers in Marine Science* 2016; **3**.
82. Heraud P, Beardall J, McNaughton D, Wood BR. In vivo prediction of the nutrient status of individual microalgal cells using Raman microspectroscopy. *FEMS Microbiology Letters* 2007; **275**: 24-30.
83. Preisner O, Lopes JA, Guiomar R, Machado J, Menezes JC. Fourier transform infrared (FT-IR) spectroscopy in bacteriology: towards a reference method for bacteria discrimination. *Analytical and bioanalytical chemistry* 2007; **387**: 1739-1748.
84. Reference deleted.
85. Dao L, Beardall J, Heraud P. Characterisation of Pb-induced changes and prediction of Pb exposure in microalgae using infrared spectroscopy. *Aquatic Toxicology* 2017; **188**: 33-42.
86. Naumann D. Infrared spectroscopy in microbiology. In: Meyers RA, editor. Encyclopedia of analytical chemistry. Chichester: John Wiley & Sons Ltd; 2000, pp 102-131.
87. Bains S, Corfield RM, Norris RD. Mechanisms of climate warming at the end of the Paleocene. *Science* 1999; **285**: 724-727.
88. Scopes A. The infrared spectra of some acetic acid bacteria. *Microbiology* 1962; **28**: 69-79.

89. Nichols PD, Henson JM, Guckert JB, Nivens DE, White DC. Fourier transform-infrared spectroscopic methods for microbial ecology: analysis of bacteria, bacteria-polymer mixtures and biofilms. *Journal of Microbiological Methods* 1985; **4**: 79-94.
90. Jarute G, Kainz A, Schroll G, Baena JR, Lendl B. On-Line Determination of the Intracellular Poly (β-hydroxybutyric acid) Content in Transformed Escherichia c oli and Glucose during PHB Production Using Stopped-Flow Attenuated Total Reflection FT-IR Spectrometry. *Analytical Chemistry* 2004; **76**: 6353-6358.
91. Blum MM, John H. Historical perspective and modern applications of attenuated total reflectance–Fourier transform infrared spectroscopy (ATR-FTIR). *Drug testing and analysis* 2012; **4**: 298-302.
92. Naumann D, Helm D, Labischinski H. Microbiological characterizations by FT-IR spectroscopy. *Nature* 1991; **351**: 81-82.
93. Helm D, Labischinski H, Naumann D. Elaboration of a procedure for identification of bacteria using Fourier-Transform IR spectral libraries: a stepwise correlation approach. *Journal of Microbiological Methods* 1991; **14**: 127-142.
94. Gautam R, Vanga S, Ariese F, Umapathy S. Review of multidimensional data processing approaches for Raman and infrared spectroscopy. *EPJ Techniques and Instrumentation* 2015; **2**: 8.
95. Perez-Guaita D, Kochan K, Martin M, Andrew DW, Heraud P, Richards JS, et al. Multimodal vibrational imaging of cells. *Vibrational spectroscopy* 2017; **91**: 46-58.
96. Lin S-Y, Li M-J, Liang R-C, Lee S-M. Non-destructive analysis of the conformational changes in human lens lipid and protein structures of the immature cataracts associated with glaucoma. *Spectrochimica Acta Part A: Molecular and Biomolecular Spectroscopy* 1998; **54**: 1509-1517.
97. Oliver SG, Winson MK, Kell DB, Baganz F. Systematic functional analysis of the yeast genome. *Trends in biotechnology* 1998; **16**: 373-378.
98. Heraud P, Wood BR, Beardall J, McNaughton D. Probing the influence of the environment on microalgae using infrared and raman spectroscopy. New approaches in biomedical spectroscopy: ACS Publications; 2007, pp 85-106.
99. Kansiz M, Heraud P, Wood B, Burden F, Beardall J, McNaughton D. Fourier transform infrared microspectroscopy and chemometrics as a tool for the discrimination of cyanobacterial strains. *Phytochemistry* 1999; **52**: 407-417.
100. Giordano M, Kansiz M, Heraud P, Beardall J, Wood B, McNaughton D. Fourier transform infrared spectroscopy as a novel tool to investigate changes in intracellular macromolecular pools in the marine microalga Chaetoceros muellerii (Bacillariophyceae). *Journal of Phycology* 2001; **37**: 271-279.
101. Beardall J, Berman T, Heraud P, Kadiri MO, Light BR, Patterson G, et al. A comparison of methods for detection of phosphate limitation in microalgae. *Aquatic sciences* 2001; **63**: 107-121.
102. Beardall J, Young E, Roberts S. Approaches for determining phytoplankton nutrient limitation. *Aquatic sciences* 2001; **63**: 44-69.
103. Heraud P, Wood BR, Tobin MJ, Beardall J, McNaughton D. Mapping of nutrient-induced biochemical changes in living algal cells using synchrotron infrared microspectroscopy. *FEMS Microbiology Letters* 2005; **249**: 219-225.
104. Wood BR, Heraud P, Stojkovic S, Morrison D, Beardall J, McNaughton D. A portable Raman acoustic levitation spectroscopic system for the identification and environmental monitoring of algal cells. *Analytical Chemistry* 2005; **77**: 4955-4961.
105. Heraud P, Wood BR, Beardall J, McNaughton D. Effects of pre-processing of Raman spectra on in vivo classification of nutrient status of microalgal cells. *Journal of Chemometrics* 2006; **20**: 193-197.
106. Martens H, Nielsen JP, Engelsen SB. Light scattering and light absorbance separated by extended multiplicative signal correction. Application to near-infrared transmission analysis of powder mixtures. *Analytical Chemistry* 2003; **75**: 394-404.
107. Geladi P. Notes on the history and nature of partial least squares (PLS) modelling. *Journal of Chemometrics* 1988; **2**: 231-246.
108. Wold S. Pattern recognition by means of disjoint principal components models. *Pattern recognition* 1976; **8**: 127-139.
109. Dean A, Martin MC, Sigee D. Resolution of codominant phytoplankton species in a eutrophic lake using synchrotron-based Fourier transform infrared spectroscopy. *Phycologia* 2007; **46**: 151-159.
110. Murdock JN, Dodds WK, Wetzel DL. Subcellular localized chemical imaging of benthic algal nutritional content via HgCdTe array FT-IR. *Vibrational spectroscopy* 2008; **48**: 179-188.

111. Heraud P, Stojkovic S, Beardall J, McNaughton D, Wood BR. Intercolonial variability in macromolecular composition in p-starved and p-replete scenedesmus populations revealed by infrared microspectroscopy. *Journal of Phycology* 2008; **44**: 1335-1339.
112. Sackett O, Armand L, Beardall J, Hill R, Doblin M, Connelly C, et al. Taxon-specific responses of Southern Ocean diatoms to Fe enrichment revealed by synchrotron radiation FTIR microspectroscopy. *Biogeosciences* 2014; **11**: 5795-5808.
113. Sackett O, Petrou K, Reedy B, De Grazia A, Hill R, Doblin M, et al. Phenotypic Plasticity of Southern Ocean Diatoms: Key to Success in the Sea Ice Habitat? *PLoS ONE* 2013; **8**: e81185.
114. Lin R, Ritz GP. Reflectance FT-IR microspectroscopy of fossil algae contained in organic-rich shales. *Applied Spectroscopy* 1993; **47**: 265-271.
115. Mann DG, Crawford RM, Round FE. Bacillariophyta. In: Archibald JM, Simpson AGB, Slamovits CH, editors. Handbook of the Protists. Cham: Springer International Publishing; 2017, pp 205-266.
116. Crawford RM, Hinz F, Honeywill C. Three species of the diatom genus corethron castracane: structure, distribution and taxonomy. *Diatom Research* 1998; **13**: 1-28.
117. Exley C, Tollervey A, Gray G, Roberts S, Birchall JD. Silicon, Aluminium and the Biological Availability of Phosphorus in Algae. *Proceedings of the Royal Society B: Biological Sciences* 1993; **253**: 93-99.
118. Gensemer RW. Role of aluminum and growth rate on changes in cell size and silica content of silica-limited populations of asterionella ralfsii var. Americana (bacillariophyceae). *Journal of Phycology* 1990; **26**: 250-258.
119. Vrieling E, Poort L, Beelen T, Gieskes W. Growth and silica content of the diatoms Thalassiosira weissflogii and Navicula salinarum at different salinities and enrichments with aluminium. *European Journal of Phycology* 1999; **34**: 307-316.
120. Guillard RR. Culture of phytoplankton for feeding marine invertebrates. Culture of marine invertebrate animals: Springer; 1975, pp 29-60.
121. Chu WL, Phang SM, Goh SH. Studies on the production of useful chemicals, especially fatty acids in the marine diatom Nitzschia conspicua Grunow. *Hydrobiologia* 1994; **285**: 33-40.
122. Hildebrand M, Frigeri LG, Davis AK. Synchronized Growth Of Thalassiosira Pseudonana (Bacillariophyceae) Provides Novel Insights Into Cell-Wall Synthesis Processes In Relation To The Cell Cycle. *Journal of Phycology* 2007; **43**: 730-740.
123. Thompson PA, Guo Mx, Harrison PJ, Whyte JN. Effects of variation in temperature. II. On the fatty acid composition of eight species of marine phytoplankton. *Journal of Phycology* 1992; **28**: 488-497.
124. Montagnes DJ, Franklin M. Effect of temperature on diatom volume, growth rate, and carbon and nitrogen content: reconsidering some paradigms. *Limnology and oceanography* 2001; **46**: 2008-2018.
125. Jebsen C, Norici A, Wagner H, Palmucci M, Giordano M, Wilhelm C. FTIR spectra of algal species can be used as physiological fingerprints to assess their actual growth potential. *Physiologia plantarum* 2012; **146**: 427-438.
126. Qiao H, Cong C, Sun C, Li B, Wang J, Zhang L. Effect of culture conditions on growth, fatty acid composition and DHA/EPA ratio of Phaeodactylum tricornutum. *Aquaculture* 2016; **452**: 311-317.
127. Lu Y, Zhou W, Wei L, Li J, Jia J, Li F, et al. Regulation of the cholesterol biosynthetic pathway and its integration with fatty acid biosynthesis in the oleaginous microalga Nannochloropsis oceanica. *Biotechnology for biofuels* 2014; **7**: 81.
128. Driver T, Bajhaiya AK, Allwood JW, Goodacre R, Pittman JK, Dean AP. Metabolic responses of eukaryotic microalgae to environmental stress limit the ability of FT-IR spectroscopy for species identification. *Algal Research* 2015; **11**: 148-155.
129. Giordano M, Olivieri C, Ratti S, Norici A, Raven JA, Knoll AH. A tale of two eras: Phytoplankton composition influenced by oceanic paleochemistry. *Geobiology* 2018; **16**: 498-506.
130. Durako MJ, Kunzelman JI. Photosynthetic characteristics of Thalassia testudinum measured in situ by pulse-amplitude modulated (PAM) fluorometry: methodological and scale-based considerations. *Aquatic Botany* 2002; **73**: 173-185.
131. L.K. Armand, P.E. O'Brien and On-board Scientific Party. 2018. Interactions of the Totten Glacier with the Southern Ocean through multiple glacial cycles (IN2017-V01): Post-survey report, Research School of Earth Sciences, Australian National University: Canberra, http://dx.doi.org/10.4225/13/5acea64c48693.

132. Liang Y, Beardall J, Heraud P. Changes in growth, chlorophyll fluorescence and fatty acid composition with culture age in batch cultures of Phaeodactylum tricornutum and Chaetoceros muelleri (Bacillariophyceae). *Botanica Marina* 2006; **49**: 165-173.
133. Robert S, Mansour MP, Blackburn SI. Metolachlor-Mediated Selection of a Microalgal Strain Producing Novel Polyunsaturated Fatty Acids. *Marine biotechnology* 2007; **9**: 146-153.
134. Claquin P, Probert I, Lefebvre S, Veron B. Effects of temperature on photosynthetic parameters and TEP production in eight species of marine microalgae. *Aquatic Microbial Ecology* 2008; **51**: 1-11.
135. Andersen RA, Phycological Society of A. *Algal culturing techniques*. Boston, Massachusetts: Elsevier/Academic Press; 2005.
136. Liu J. Optimisation of biomass and lipid production by adjusting the interspecific competition mode of Dunaliella salina and Nannochloropsis gaditana in mixed culture. *Journal of Applied Phycology* 2014; **26**: 163-171.
137. Jacques G. Some ecophysiological aspects of the Antarctic phytoplankton. *Polar Biology* 1983; **2**: 27-33.
138. Eilers P, Peeters J. A model for the relationship between light intensity and the rate of photosynthesis in phytoplankton. *Ecological modelling* 1988; **42**: 199-215.
139. Goss R, Lepetit B. Biodiversity of NPQ. *Journal of Plant Physiology* 2015; **172**: 13-32.
140. Horton P. Molecular design of the photosystem II light-harvesting antenna: photosynthesis and photoprotection. *Journal of Experimental Botany* 2004; **56**: 365-373.
141. Genty B, Briantais J-M, Baker NR. The relationship between the quantum yield of photosynthetic electron transport and quenching of chlorophyll fluorescence. *Biochimica et Biophysica Acta* 1989; **990**: 87-92.
142. Maxwell K, Johnson GN. Chlorophyll fluorescence—a practical guide. *Journal of Experimental Botany* 2000; **51**: 659-668.
143. Kromkamp JC, Forster RM. The use of variable fluorescence measurements in aquatic ecosystems: differences between multiple and single turnover measuring protocols and suggested terminology. *European Journal of Phycology* 2003; **38**: 103-112.
144. Kiernan J. Histological and Histochemical Methods Theory and Practice. Department of Anatomy. Canada: Pergamon Press; 1981.
145. Mason JT, O'leary TJ. Effects of formaldehyde fixation on protein secondary structure: a calorimetric and infrared spectroscopic investigation. *Journal of Histochemistry & Cytochemistry* 1991; **39**: 225-229.
146. Zohdi V, Whelan DR, Wood BR, Pearson JT, Bambery KR, Black MJ. Importance of Tissue Preparation Methods in FTIR Micro-Spectroscopical Analysis of Biological Tissues: 'Traps for New Users'. *PLoS ONE* 2015; **10**: e0116491.
147. Faolain EO, Hunter MB, Byrne JM, Kelehan P, McNamara M, Byrne HJ, et al. A study examining the effects of tissue processing on human tissue sections using vibrational spectroscopy. *Vibrational spectroscopy* 2005; **38**: 121-127.
148. Hastings G, Wang R, Krug P, Katz D, Hilliard J. Infrared microscopy for the study of biological cell monolayers. I. Spectral effects of acetone and formalin fixation. *Biopolymers* 2008; **89**: 921-930.
149. Domenighini A, Giordano M. Fourier transform infrared spectroscopy of microalgae as a novel tool for biodiversity studies, species identification, and the assessment of water quality. *Journal of Phycology* 2009; **45**: 522-531.
150. Mayers JJ, Flynn KJ, Shields RJ. Rapid determination of bulk microalgal biochemical composition by Fourier-Transform Infrared spectroscopy. *Bioresource Technology* 2013; **148**: 215-220.
151. Vongsvivut J, Heraud P, Gupta A, Puri M, McNaughton D, Barrow CJ. FTIR microspectroscopy for rapid screening and monitoring of polyunsaturated fatty acid production in commercially valuable marine yeasts and protists. *Analyst* 2013; **138**: 6016-6031.
152. Karpinska J. Basic principles and analytical application of derivative spectrophotometry. In: U J, editor. Macro To Nano Spectroscopy: InTech, Rijekz; 2012, pp.
153. Tillmann U, Baumann MEM, Aletsee L. Distribution of carbon among photosynthetic end products in the bloom-forming arctic diatom Thalassiosira antarctica COMBER. *Polar Biology* 1989; **10**: 231-238.
154. Baranska M. *Optical spectroscopy and computational methods in biology and medicine*. Baranska M, editor. Dordrecht, New York: Springer; 2014.

155. Kröger N, Poulsen N. Diatoms—from cell wall biogenesis to nanotechnology. *Annu Rev Genetics* 2008; **42**.
156. Dean AP, Sigee DC, Estrada B, Pittman JK. Using FTIR spectroscopy for rapid determination of lipid accumulation in response to nitrogen limitation in freshwater microalgae. *Bioresource Technology* 2010; **101**: 4499-4507.
157. Miglio R, Palmery S, Salvalaggio M, Carnelli L, Capuano F, Borrelli R. Microalgae triacylglycerols content by FT-IR spectroscopy. *Journal of Applied Phycology* 2013; **25**: 1621-1631.
158. Parkhill JP, Maillet G, Cullen JJ. Fluorescence-based maximal quantum yield for PSII as a diagnostic of nutrient stress. *Journal of Phycology* 2001; **37**: 517-529.
159. El-Sayed SZ, Taguchi S. Primary production and standing crop of phytoplankton along the ice-edge in the Weddell Sea. *Deep Sea Research Part A Oceanographic Research Papers* 1981; **28**: 1017-1032.
160. Paerl HW. Mitigating harmful cyanobacterial blooms in a human-and climatically-impacted world. *Life* 2014; **4**: 988-1012.
161. Armand LK, Crosta X, Romero O, Pichon J-J. The biogeography of major diatom taxa in Southern Ocean sediments: 1. Sea ice related species. *Palaeogeography, Palaeoclimatology, Palaeoecology* 2005; **223**: 93-126.
162. Lizotte MP. The Contributions of Sea Ice Algae to Antarctic Marine Primary Production1. *American Zoologist* 2001; **41**: 57-73.
163. Guschina IA, Harwood JL. Lead and copper effects on lipid metabolism in cultured lichen photobionts with different phosphorus status. *Phytochemistry* 2006; **67**: 1731-1739.
164. Lancelot C, Mathot S. Biochemical fractionation of primary production by phytoplankton in Belgian coastal waters during short-and long-term incubations with 14C-bicarbonate. *Marine Biology* 1985; **86**: 219-226.
165. Ramachandra T, Mahapatra D, Karthick B. Milking Diatoms for Sustainable Energy: Biochemical Engineering versus Gasoline-Secreting Diatom Solar Panels. *Industrial & Engineering Chemistry Research* 2009; **48**: 8769-8788.
166. Dunahay TG, Jarvis EE, Dais SS, Roessler PG. Manipulation of microalgal lipid production using genetic engineering. *Applied Biochemistry and Biotechnology* 1996; **57**: 223.
167. Maeda Y, Nojima D, Yoshino T, Tanaka T. Structure and properties of oil bodies in diatoms. *Philosophical Transactions of the Royal Society B: Biological Sciences* 2017; **372**.
168. Wilhelm C, Büchel C, Fisahn J, Goss R, Jakob T, LaRoche J, et al. The regulation of carbon and nutrient assimilation in diatoms is significantly different from green algae. *Protist* 2006; **157**: 91-124.
169. Morgan-Kiss R, Ivanov AG, Williams J, Mobashsher K, Huner NPA. Differential thermal effects on the energy distribution between photosystem II and photosystem I in thylakoid membranes of a psychrophilic and a mesophilic alga. *Biochimica et Biophysica Acta* 2002; **1561**: 251-265.
170. Mock T, Kroon BM. Photosynthetic energy conversion under extreme conditions—II: the significance of lipids under light limited growth in Antarctic sea ice diatoms. *Phytochemistry* 2002; **61**: 53-60.
171. Bidigare RR, Ondrusek ME, Kennicutt II MC, Ituurriaga R, Harvey HR, Hoham RW, et al. Evidence for a photoprotective function for secondary carotenoids of snow algae. *Journal of Phycology* 1993; **29**.
172. Mock T, Kroon BMA. Photosynthetic energy conversion under extreme conditions—I: important role of lipids as structural modulators and energy sink under N-limited growth in Antarctic sea ice diatoms. *Phytochemistry* 2002; **61**: 41-51.
173. Murata N, Wada H. Acyl-lipid desaturases and their importance in the tolerance and acclimatization to cold of cyanobacteria. *Biochemical Journal* 1995; **308**: 1-8.
174. Morgan-Kiss RM, Priscu JC, Pocock T, Gudynaite-Savitch L, Huner NP. Adaptation and acclimation of photosynthetic microorganisms to permanently cold environments. *Microbiology and molecular biology reviews* 2006; **70**: 222-252.
175. Descolas-Gros C, de Billy G. Temperature adaptation of RuBP carboxylase: kinetic properties in marine Antarctic diatoms. *Journal of Experimental Marine Biology and Ecology* 1987; **108**: 147-158.
176. Devos N, Ingouff M, Loppes R, Matagne RF. RUBISCO adaptation to low temperatures: a comparative study in psychrophilic and mesophilic unicellular algae. *Journal of Phycology* 1998; **34**: 655-660.
177. Laskowski RA. PDBsum: summaries and analyses of PDB structures. *Nucleic acids research* 2001; **29**: 221-222.

178. Napolitano MJ, Shain DH. Distinctions in adenylate metabolism among organisms inhabiting temperature extremes. *Extremophiles* 2005; **9**: 93-98.
179. Maxwell DP, Falk S, Trick CG, Huner NP. Growth at low temperature mimics high-light acclimation in Chlorella vulgaris. *Plant physiology* 1994; **105**: 535-543.
180. Foyer C, Furbank R, Harbinson J, Horton P. The mechanisms contributing to photosynthetic control of electron transport by carbon assimilation in leaves. *Photosynthesis Research* 1990; **25**: 83-100.
181. Kroon BM, Thoms S. From electron to biomass: a mechanistic model to describe phytoplankton photosynthesis and steady-state growth rates. *Journal of Phycology* 2006; **42**: 593-609.
182. Paul GF, Cara W. Phytoplankton productivity? *Nature* 1993; **362**: 796.
183. Nicol S, Pauly T, Bindoff NL, Wright S, Thiele D, Hosie GW, et al. Ocean circulation off east Antarctica affects ecosystem structure and sea-ice extent. *Nature* 2000; **406**: 504.
184. Lasbleiz M, Leblanc K, Blain S, Ras J, Cornet-Barthaux V, Hélias Nunige S, et al. Pigments, elemental composition (C, N, P, and Si), and stoichiometry of particulate matter in the naturally iron fertilized region of Kerguelen in the Southern Ocean. *Biogeosciences* 2014; **11**: 5931-5955.
185. Fahl K, Kattner G. Lipid content and fatty acid composition of algal communities in sea-ice and water from the Weddell Sea (Antarctica). *Polar Biology* 1993; **13**: 405-409.
186. Lohrenz SE, Taylor CD. Primary production of protein: I. Comparison of net cellular carbon and protein synthesis with 14C-derived rate estimates in steady-state cultures of marine phytoplankton. *Mar Ecol Prog Ser* 1987; **35**: 277-292.
187. Pond DW, Priddle J, Sargent JR, Watkins JL. Laboratory studies of assimilation and egestion of algal lipid by Antarctic krill—methods and initial results. *Journal of Experimental Marine Biology and Ecology* 1995; **187**: 253-268.
188. Hessen DO, Ågren GI, Anderson TR, Elser JJ, De Ruiter PC. Carbon sequestration in ecosystems: the role of stoichiometry. *Ecology* 2004; **85**: 1179-1192.
189. Arrigo KR. Marine microorganisms and global nutrient cycles. *Nature* 2004; **437**: 349.
190. Finkel ZV, Beardall J, Flynn KJ, Quigg A, Rees TAV, Raven JA. Phytoplankton in a changing world: cell size and elemental stoichiometry. *Journal of Plankton Research* 2010; **32**: 119-137.
191. Litchman E, Klausmeier CA, Schofield OM, Falkowski PG. The role of functional traits and trade-offs in structuring phytoplankton communities: scaling from cellular to ecosystem level. *Ecology Letters* 2007; **10**: 1170-1181.
192. Benoiston A-S, Ibarbalz FM, Bittner L, Guidi L, Jahn O, Dutkiewicz S, et al. The evolution of diatoms and their biogeochemical functions. *Philosophical Transactions of the Royal Society B: Biological Sciences* 2017; **372**.
193. Claquin P, Martin-Jézéquel V, Kromkamp JC, Veldhuis MJ, Kraay GW. Uncoupling of silicon compared with carbon and nitrogen metabolisms and the role of the cell cycle in continuous cultures of thalassiosira pseudonana (bacillariophyceae) under light, nitrogen, and phosphorus control. *Journal of Phycology* 2002; **38**: 922-930.
194. Raven J, Waite A. The evolution of silicification in diatoms: inescapable sinking and sinking as escape? *New Phytologist* 2004; **162**: 45-61.
195. Wilken S, Huisman J, Naus-Wiezer S, Van Donk E. Mixotrophic organisms become more heterotrophic with rising temperature. *Ecology Letters* 2013; **16**: 225-233.
196. Neori A, Holm-Hansen O. Effect of temperature on rate of photosynthesis in Antarctic phytoplankton. *Polar Biology* 1982; **1**: 33-38.

Supplementary material

Table S1. Raw cell count data (part 1)

Spp.	Vessel No.	Day	Temp	Date	Time	Count 1	Count 2	Count 3	Count 4	Count 5	Count 6	Count 7	avg. x 10000	SD
C	1	1	3	25-Apr	11:00	2	4	3	14	10	5		6.3	4.7
C	3	1	3	25-Apr	11:00	7	7	6	4	5	13		7.0	3.2
C	8	1	3	25-Apr	11:00	10	11	5	20	5	8		9.8	5.6
F	2	1	3	25-Apr	11:00	8	8	12	9	16	13		11.0	3.2
F	6	1	3	25-Apr	11:00	13	12	8	11	8	18		11.7	3.7
F	7	1	3	25-Apr	11:00	9	9	11	9	15	12		10.8	2.4
C	1	2	3	26-Apr	11:50	18	5	12	6	12	8		10.2	4.8
C	3	2	3	26-Apr	11:50	6	10	8	7	12	10		8.8	2.2
C	8	2	3	26-Apr	11:50	8	8	9	13	23	8		11.5	6.0
F	2	2	3	26-Apr	11:50	9	24	31	60	21	17		27.0	17.7
F	6	2	3	26-Apr	11:50	28	40	22	29	13			26.4	9.9
F	7	2	3	26-Apr	11:50	5	10	8	10	5	7		7.5	2.3
C	1	3	3	27-Apr	10:00	12	22	20	12	16	10		15.3	4.8
C	3	3	3	27-Apr	10:00	12	21	16	19	18	20		17.7	3.3
C	8	3	3	27-Apr	10:00	10	19	25	28	15	17		19.0	6.6
F	2	3	3	27-Apr	10:00	7	13	15	15	12	9		11.8	3.3
F	6	3	3	27-Apr	10:00	14	16	21	18	10	23		17.0	4.7
F	7	3	3	27-Apr	10:00	7	16	12	18	6	12		11.8	4.8
C	1	4	3	28-Apr	12:00	25	25	32	21	18	21		23.7	4.9
C	3	4	3	28-Apr	12:00	34	47	51	41	28	19		36.7	12.0
C	8	4	3	28-Apr	12:00	38	50	72	42	26	29		42.8	16.7
F	2	4	3	28-Apr	12:00	42	33	16	22	22	27		27.0	9.3
F	6	4	3	28-Apr	12:00	16	21	22	22	24	16		20.2	3.4
F	7	4	3	28-Apr	12:00	26	19	13	14	25	24		20.2	5.7
C	1	6	3	30-Apr	8:30	39	28	39	35	17	31		31.5	8.3
C	3	6	3	30-Apr	8:30	42	45	56	56	56	39	31	46.4	9.9
C	8	6	3	30-Apr	8:30	57	40	55	48	54	53		51.2	6.2
F	2	6	3	30-Apr	8:30	21	10	7	19	19	8	13	13.9	5.8
F	6	6	3	30-Apr	8:30	10	20	10	20	24	17		16.8	5.7
F	7	6	3	30-Apr	8:30	15	14	15	12	21	19		16.0	3.3
C	1	7	3	1-May	10:30	41	67	52	64	47	47		53.0	10.3
C	3	7	3	1-May	10:30	47	45	57	70	56	77		58.7	12.6
C	8	7	3	1-May	10:30	73	87	73	68	76	86		77.2	7.7
F	2	7	3	1-May	10:30	21	24	26	30	18	28		24.5	4.5
F	6	7	3	1-May	10:30	41	33	33	29	31	46		35.5	6.6
F	7	7	3	1-May	10:30	19	6	18	15	25	28	21	18.9	7.2
C	1	8	3	2-May	10:30	88	92	99	127	93	93		98.7	14.3
C	3	8	3	2-May	10:30	66	77	103	94	76	78		82.3	13.5
C	8	8	3	2-May	10:30	122	144	137	134	143	135		135.8	7.9
F	2	8	3	2-May	10:30	30	37	33	20	23	9	15	23.9	10.1
F	6	8	3	2-May	10:30	50	52	69	42	55	61		54.8	9.3
F	7	8	3	2-May	10:30	20	24	46	32	32	25		29.8	9.2
C	1	9	3	3-May	10:00	116	190	181	167	167	132		158.8	28.8
C	3	9	3	3-May	10:00	133	156	162	184	115	171		153.5	25.4
C	8	9	3	3-May	10:00	204	226	210	195	201	199		205.8	11.1
F	2	9	3	3-May	10:00	43	59	59	38	67	63		54.8	11.6
F	6	9	3	3-May	10:00	88	112	128	100	108	108		107.3	13.2
F	7	9	3	3-May	10:00	55	57	52	69	65	72		61.7	8.1
C	1	10	3	4-May	10:30	150	163	153	155	157	168		157.7	6.7
C	3	10	3	4-May	10:30	122	132	107	113	113	116		117.2	8.8
C	8	10	3	4-May	10:30	164	195	181	138	150	157		164.2	20.8
F	2	10	3	4-May	10:30	107	78	77	101	72	78		85.5	14.6
F	6	10	3	4-May	10:30	89	85	101	100	109	100		97.3	8.8

C = *Corethron pennatum*, F = *Flagilariopsis sp*. (which was excluded from experiments during pilot trial)

Table S1. Raw cell count data (part 2)

Spp.	Vessel No.	Day	Temp	Date	Time	Count 1	Count 2	Count 3	Count 4	Count 5	Count 6	Count 7	avg. x 10000	SD
F	7	10	3	4-May	10:30	91	83	93	80	109	110		94.3	12.7
C	1	11	3	5-May	14:00	83	99	108	118	121	91		103.3	15.1
C	3	11	3	5-May	14:00	83	98	95	95	92	79		90.3	7.6
C	8	11	3	5-May	14:00	119	121	135	138	127	108		124.7	11.1
F	2	11	3	5-May	14:00	65	73	60	86	74	63		70.2	9.5
F	6	11	3	5-May	14:00	112	124	92	87	109	103		104.5	13.6
F	7	11	3	5-May	14:00	83	64	82	80	76	88		78.8	8.3
C	1	1	3	6-May	14:00	34	48	41	33	35	40		38.5	5.7
C	6	1	3	6-May	14:00	42	41	45	44	41	47		43.3	2.4
F	7	1	3	6-May	14:00	34	30	33	23	18	22		26.7	6.6
C	8	1	3	6-May	14:00	43	36	46	55	26	40		41.0	9.8
C	1	1	5	6-May	14:00	40	27	38	53	41	41		40.0	8.3
C	3	1	5	6-May	14:00	33	44	38	45	45	34		39.8	5.6
C	5	1	5	6-May	14:00	34	36	46	38	30	26		35.0	6.9
F	6	1	5	6-May	14:00	25	20	27	30	32	26		26.7	4.2
C	1	2	3	7-May	16:00	51	71	63	69	64	49		61.2	9.2
C	6	2	3	7-May	16:00	76	75	93	67	72	87		78.3	9.8
F	7	2	3	7-May	16:00	32	45	44	39	38	53		41.8	7.2
C	8	2	3	7-May	16:00	71	84	83	62	56	46		67.0	15.2
C	1	2	5	7-May	16:00	50	63	70	70	50	51		59.0	9.8
C	3	2	5	7-May	16:00	50	69	58	57	66	53		58.8	7.4
C	5	2	5	7-May	16:00	63	62	51	41	58	46		53.5	9.0
F	6	2	5	7-May	16:00	45	40	48	47	48	48		46.0	3.2
C	1	3	3	8-May	14:00	108	104	123	91	110	94		105.0	11.6
C	6	3	3	8-May	14:00	104	125	121	138	118	106		118.7	12.6
F	7	3	3	8-May	14:00	72	78	103	73	74	69		78.2	12.5
C	8	3	3	8-May	14:00	71	95	104	92	88	93		90.5	10.9
C	1	3	5	8-May	14:00	62	90	92	78	78	72		78.7	11.2
C	3	3	5	8-May	14:00	75	83	95	80	101	76		85.0	10.6
C	5	3	5	8-May	14:00	97	84	76	73	82	86		83.0	8.4
F	6	3	5	8-May	14:00	87	92	80	58	64	67		74.7	13.6
C	1	4	3	9-May	9:00	112	129	118	96	135	131		120.2	14.6
C	6	4	3	9-May	9:00	138	148	114	106	138	107		125.2	18.3
C	8	4	3	9-May	9:00	93	111	128	121	120	104		112.8	12.8
C	1	4	5	9-May	9:00	89	85	75	86	111	77		87.2	12.9
C	3	4	5	9-May	9:00	82	81	70	83	71	93		80.0	8.5
C	5	4	5	9-May	9:00	98	87	86	108	85	91		92.5	9.0
C	1	1	3	10-May	11:30	53	42	45	53	41	44		46.3	5.4
C	6	1	3	10-May	11:30	63	68	85	59	55	63		65.5	10.5
C	8	1	3	10-May	11:30	48	38	47	50	55	34		45.3	7.8
C	1	1	5	10-May	11:30	62	41	55	60	44			52.4	9.4
C	3	1	5	10-May	11:30	48	61	47	66	56	49		54.5	7.8
C	5	1	5	10-May	11:30	59	57	54	44	35	44		48.8	9.3
C	1	2	3	11-May	15:30	77	68	90	73	69	68		74.2	8.5
C	6	2	3	11-May	15:30	131	107	112	118	91	96		109.2	14.6
C	8	2	3	11-May	15:30	70	79	78	75	63	70		72.5	6.0
C	1	2	5	11-May	15:30	59	63	73	58	59	68		63.3	6.0
C	3	2	5	11-May	15:30	88	96	83	69	78	88		83.7	9.4
C	5	2	5	11-May	15:30	55	64	65	63	73	60		63.3	6.0
C	1	3	3	12-May	11:00	75	84	102	106	100	75		90.3	14.0
C	6	3	3	12-May	11:00	100	103	122	134	126	116		116.8	13.3
C	8	3	3	12-May	11:00	123	105	93	109	123	121		112.3	12.2
C	1	3	5	12-May	11:00	56	58	48	62	73	62		59.8	8.3

Table S1. Raw cell count data (part 3)

Spp.	Vessel No.	Day	Temp	Date	Time	Count 1	Count 2	Count 3	Count 4	Count 5	Count 6	Count 7	avg. x 10000	SD
C	3	3	5	12-May	11:00	69	68	78	80	69	62		71.0	6.8
C	5	3	5	12-May	11:00	50	59	47	46	51	52		50.8	4.6
C	1	1	3	13-May	17:00	34	56	51	65	57	62		54.2	11.0
C	6	1	3	13-May	17:00	50	62	58	63	57	55		57.5	4.8
C	8	1	3	13-May	17:00	26	41	43	28	38	38		35.7	7.0
C	1	1	5	13-May	17:00	27	37	39	24	42	36		34.2	7.1
C	3	1	5	13-May	17:00	25	20	32	31	32	22		27.0	5.4
C	5	1	5	13-May	17:00	33	41	45	36	39	33		37.8	4.8
C	1	2	3	14-May	15:30	81	83	76	73	62	71		74.3	7.6
C	6	2	3	14-May	15:30	108	110	107	106	117	105		108.8	4.4
C	8	2	3	14-May	15:30	55	83	54	62	79	66	81	68.6	12.4
C	1	2	5	14-May	15:30	46	41	35	55	70	55	55	51.0	11.5
C	3	2	5	14-May	15:30	49	31	34	41	39	22	29	35.0	8.9
C	5	2	5	14-May	15:30	48	76	43	58	52	38	49	52.0	12.3
C	1	3	3	15-May	3:30	86	77	79	89	67	77		79.2	7.8
C	6	3	3	15-May	3:30	111	103	114	103	102	110		107.2	5.1
C	8	3	3	15-May	3:30	80	67	85	86	71	65		75.7	9.2
C	1	4	5	16-May	18:00	21	23	30	44	36	23		29.5	9.0
C	3	4	5	16-May	18:00	46	66	59	48	67	64		58.3	9.2
C	5	4	5	16-May	18:00	39	39	30	30	24	29		31.8	6.0
C	5	1	3	30-May	17:45	15	39	28	19	39	27		27.8	9.9
C	6	1	1.5	30-May	17:45	10	16	16	16	19	19		16.0	3.3
C	7	1	1.5	30-May	17:45	14	26	13	25	25	15		19.7	6.3
C	5	2	3	31-May	15:30	39	26	28	37	19	23		28.7	7.9
C	6	2	1.5	31-May	15:30	30	16	27	30	32	32		27.8	6.1
C	7	2	1.5	31-May	15:30	40	22	35	39	31	30		32.8	6.7
C	6	3	1.5	1-Jun	16:00	34	34	46	35	41	34		37.3	5.0
C	7	3	1.5	1-Jun	16:00	37	39	41	45	52	48		43.7	5.7
C	5	3	3	1-Jun	16:00	47	45	38	46	40	35		41.8	4.9
C	1	3	1.5	1-Jun	16:00	66	57	58	56	59	62		59.7	3.7
C	3	3	3	1-Jun	16:00	52	65	48	48	66	61		56.7	8.3
C	4	1	1.5	2-Jun	12:30	29	36	41	26	35	39		34.3	5.8
C	6	1	1.5	2-Jun	12:30	16	31	32	22	20			24.2	7.0
C	7	1	1.5	2-Jun	12:30	27	24	30	22	25	22		25.0	3.1
C	5	1	3	2-Jun	12:30	24	21	28	15	29	11		21.3	7.2
C	8	1	3	2-Jun	12:30	22	25	16	18	16	35		22.0	7.3
C	4	2	1.5	3-Jun	15:30	59	66	70	63	69	60		64.5	4.6
C	6	2	1.5	3-Jun	15:30	31	41	27	34	39	29		33.5	5.6
C	7	2	1.5	3-Jun	15:30	24	21	28	21	40	31		27.5	7.3
C	5	2	3	3-Jun	15:30	41	30	31	28	32	40		33.7	5.5
C	8	2	3	3-Jun	15:30	38	51	48	41	39	36		42.2	6.0
C	4	3	1.5	4-Jun	20:40	82	98	78	87	78	84		84.5	7.5
C	6	3	1.5	4-Jun	20:40	85	82	68	66	70	61		72.0	9.4
C	7	3	1.5	4-Jun	20:40	82	67	82	72	53	85		73.5	12.2
C	5	3	3	4-Jun	20:40	62	61	56	67	80	52		63.0	9.8
C	8	3	3	4-Jun	20:40	72	80	66	68	76	54		69.3	9.1
C	4	1	1.5	5-Jun		46	53	36	39	43	37		42.3	6.4
C	6	1	1.5	5-Jun		24	41	34	32	26	35		32.0	6.2
C	7	1	1.5	5-Jun		42	30	41	25	39	40		36.2	7.0
C	6	1	3	5-Jun		50	33	26	34	42	32		36.2	8.5
C	8	1	3	5-Jun		34	50	45	49	27	45		41.7	9.2
C	4	2	1.5	6-Jun										
C	6	2	1.5	6-Jun		37	43	51	57	55	37		46.7	8.9

Table S1. Raw cell count data (part 4)

Spp.	Vessel No.	Day	Temp	Date	Time	Count 1	Count 2	Count 3	Count 4	Count 5	Count 6	Count 7	avg. x 10000	SD
C	7	2	1.5	6-Jun		34	45	41	44	50	47		43.5	5.5
C	6	2	3	6-Jun		64	65	57	66	68	71		65.2	4.7
C	8	2	3	6-Jun		51	70	61	55	72	74		63.8	9.6
C	4	3	1.5	7-Jun		118	102	140	126	92	97		112.5	18.7
C	6	3	1.5	7-Jun		83	104	119	87	95	91		96.5	13.2
C	7	3	1.5	7-Jun		115	97	122	104	102	89		104.8	12.0
C	6	3	3	7-Jun		96	111	92	103	100	131		105.5	14.1
C	8	3	3	7-Jun		116	108	125	126	104	104		113.8	10.0
C	4	1	1.5	8-Jun	13:30	54	53	56	70	53	49		55.8	7.3
C	6	1	1.5	8-Jun	13:30	37	43	36	39	38	32		37.5	3.6
C	7	1	1.5	8-Jun	13:30	59	41	50	73	65	53		56.8	11.4
C	6	1	3	8-Jun	13:30	51	48	72	52	61	73		59.5	11.0
C	7	1	3	8-Jun	13:30	51	61	39	70	61	41		53.8	12.3
C	8	1	3	8-Jun	13:30	42	56	50	67	56	56		54.5	8.2
C	4	2	1.5	9-Jun	14:45	111	132	112	121	105	111		115.3	9.6
C	6	2	1.5	9-Jun	14:45	85	110	95	73	86	76		87.5	13.5
C	7	2	1.5	9-Jun	14:45	93	90	100	117	88	78		94.3	13.2
C	6	2	3	9-Jun	14:45	93	81	80	74	83	68		79.8	8.5
C	7	2	3	9-Jun	14:45	95	93	79	122	93	104		97.7	14.4
C	8	2	3	9-Jun	14:45	84	99	112	82	112	101		98.3	13.1
C	4	3	1.5	10-Jun	17:43	136	171	139	149	166	119		146.7	19.5
C	6	3	1.5	10-Jun	16:30	143	130	180	152	136	128		144.8	19.4
C	7	3	1.5	10-Jun	17:13	163	156	151	149	170	141		155.0	10.4
C	6	3	3	10-Jun	14:25	152	152	197	149	130	156		156.0	22.1
C	7	3	3	10-Jun	15:45	175	165	155	179	139	167		163.3	14.6
C	8	3	3	10-Jun	15:09	130	137	143	139	123	144		136.0	8.1
C	5	1	0	11-Jun	Counts not taken									
C	6	1	0	11-Jun	Counts not taken									
C	2	1	4.5	11-Jun	Counts not taken									
C	4	1	4.5	11-Jun	Counts not taken									
C	7	1	4.5	11-Jun	Counts not taken									
C	5	2	0	12-Jun	17:30	121	137	121	120	90	133		120.3	16.5
C	6	2	0	12-Jun	17:30	116	102	101	118	134	118		114.8	12.2
C	2	2	4.5	12-Jun	17:30	136	134	116	159	112	120		129.5	17.4
C	4	2	4.5	12-Jun	17:30	139	116	132	142	104	123		126.0	14.5
C	7	2	4.5	12-Jun	17:30	130	104	125	127	129	122		122.8	9.7
C	5	3	0	13-Jun	12:25	174	155	121	147	149	161		151.2	17.7
C	6	3	0	13-Jun	12:25	158	138	138	159	141	149		147.2	9.7
C	2	3	4.5	13-Jun	12:25	180	153	176	161	193	172		172.5	14.2
C	4	3	4.5	13-Jun	12:25	143	159	148	137	154	141		147.0	8.3
C	7	3	4.5	13-Jun	12:25	125	145	116	136	144	126		132.0	11.6
C	5	1	0	14-Jun	16:00	96	110	117	95	71	122		101.8	18.6
C	6	1	0	14-Jun	16:00	90	64	84	83	85	83		81.5	9.0
C	8	1	0	14-Jun	16:00	87	87	84	105	75	87		87.5	9.8
C	2	1	4.5	14-Jun	16:00	128	124	123	101	139	139		125.7	14.0
C	4	1	4.5	14-Jun	16:00	84	85	61	79	60	58		71.2	12.8
C	7	1	4.5	14-Jun	16:00	80	99	77	81	76	78		81.8	8.6
C	5	2	0	15-Jun	16:20	155	143	166	142	139	159		150.7	10.9
C	6	2	0	15-Jun	16:20									
C	8	2	0	15-Jun	16:20	119	116	108	120	120	103		114.3	7.2
C	2	2	4.5	15-Jun	16:20	169	148	156	152	172	160		159.5	9.5
C	4	2	4.5	15-Jun	16:20	143	134	143	138	161	141		143.3	9.3
C	7	2	4.5	15-Jun	16:20	131	137	161	169	159	141		149.7	15.3

Table S1. Raw cell count data (part 5)

Spp.	Vessel No.	Day	Temp	Date	Time	Count 1	Count 2	Count 3	Count 4	Count 5	Count 6	Count 7	avg. x 10000	SD
C	5	3	0	16-Jun	14:00	180	183	178	163	166	159		171.5	10.1
C	6	3	0	16-Jun	14:00	106	102	100	107	120	115		108.3	7.7
C	8	3	0	16-Jun	14:00									
C	2	3	4.5	16-Jun	14:00	182	180	152	182	176	178		175.0	11.5
C	4	3	4.5	16-Jun	14:00	154	159	144	156	150	172		155.8	9.5
C	7	3	4.5	16-Jun	14:00	145	174	172	151	141	145		154.7	14.6
C	5	1	0	17-Jun	15:45	73	61	52	72	63	62		63.8	7.8
C	6	1	0	17-Jun	15:45	71	41	73	69	42	59		59.2	14.5
C	8	1	0	17-Jun	15:45	79	66	69	58	67	66		67.5	6.8
C	2	1	4.5	17-Jun	15:45	43	67	55	69	57	54		57.5	9.5
C	4	1	4.5	17-Jun	15:45	72	49	76	75	50	69		65.2	12.4
C	7	1	4.5	17-Jun	15:45	33	16	29	29	33	30			
C	5	2	0	18-Jun	18:00	82	96	102	124	135	88		104.5	20.8
C	6	2	0	18-Jun	18:00	95	116	118	108	111	103		108.5	8.5
C	8	2	0	18-Jun	18:00	68	132	85	96	114	89		97.3	22.6
C	2	2	4.5	18-Jun	18:00	78	115	104	127	112	143		113.2	21.9
C	4	2	4.5	18-Jun	18:00	121	153	144	142	126	142		138.0	12.0
C	7	2	4.5	18-Jun	18:00									
C	5	3	0	19-Jun	16:10	161	143	139	162	155	167		154.5	11.2
C	6	3	0	19-Jun	16:10	136	157	123	141	126	139		137.0	12.1
C	8	3	0	19-Jun	16:10	89	86	97	93	116	104		97.5	11.0
C	2	3	4.5	19-Jun	16:10									
C	4	3	4.5	19-Jun	16:10	151	137	157	143	120	137		140.8	12.9
C	7	3	4.5	19-Jun	16:10									
C	5	1	0	20-Jun	16:45	48	50	61	51	35	46		48.5	8.4
C	6	1	0	20-Jun	16:45	56	55	51	69	60	37		54.7	10.6
C	8	1	0	20-Jun	16:45	48	53	59	39	58	53		51.7	7.4
C	2	1	4.5	20-Jun	16:45	57	77	55	69	60	55		62.2	9.0
C	4	1	4.5	20-Jun	16:45	72	65	51	63	63	73		64.5	7.9
C	7	1	4.5	20-Jun	16:45	56	64	68	74	73	58		65.5	7.5
C	5	2	0	21-Jun	16:15	77	76	71	72	84	76		76.0	4.6
C	6	2	0	21-Jun	16:15	105	108	98	87	98	93		98.2	7.7
C	8	2	0	21-Jun	16:15	66	125	103	85	84	91		92.3	20.0
C	2	2	4.5	21-Jun	16:15	107	118	101	122	78	101		104.5	15.6
C	4	2	4.5	21-Jun	16:15	105	111	116	103	107	95		106.2	7.2
C	7	2	4.5	21-Jun	16:15	122	133	123	144	107	97		121.0	17.0
C	5	3	0	22-Jun	14:45	122	129	123	127	117	112		121.7	6.3
C	6	3	0	22-Jun	15:30	149	145	164	152	154	132		149.3	10.6
C	8	3	0	22-Jun	14:20	147	136	119	132	131	126		131.8	9.5
C	2	3	4.5	22-Jun	17:20	149	135	147	121	151	152		142.5	12.2
C	4	3	4.5	22-Jun	16:51	158	180	209	166	179	184		179.3	17.5
C	7	3	4.5	22-Jun	17:55	168	195	151	189	144	145		165.3	22.5

Example of RStudio script and output:

```
setwd("C:/Users/Peta Vine/Dropbox/Statistics/R Files")
alpha<-read.csv("alpha.csv")
head(alpha)
summary(alpha)
typeof(alpha)
plot(alpha$Temp,alpha$alpha)
alpha.model<-aov(alpha~Temp,data=alpha)
plot(alpha.model)
help(aov)
anova(alpha.model)
TukeyHSD(alpha.model)
```

```
Analysis of Variance Table

Response: alpha
          Df    Sum Sq    Mean Sq F value   Pr(>F)
Temp       3 0.0044327 0.00147756  10.726 0.003546 **
Residuals  8 0.0011020 0.00013775
---
Signif. codes:  0 ‘***’ 0.001 ‘**’ 0.01 ‘*’ 0.05 ‘.’ 0.1 ‘ ’ 1
```

```
  Tukey multiple comparisons of means
    95% family-wise confidence level

Fit: aov(formula = alpha ~ Temp, data = alpha)

$Temp
                       diff         lwr            upr     p adj
1.5 °C-0 °C    -0.022333333 -0.05302138  0.0083547131 0.1698629
3 °C-0 °C      -0.017666667 -0.04835471  0.0130213798 0.3219564
4.5 °C-0 °C    -0.053333333 -0.08402138 -0.0226452869 0.0023683
3 °C-1.5 °C     0.004666667 -0.02602138  0.0353547131 0.9598480
4.5 °C-1.5 °C -0.031000000 -0.06168805 -0.0003119536 0.0477627
4.5 °C-3 °C    -0.035666667 -0.06635471 -0.0049786202 0.0242794
```

Figure S1. Average second derivative spectra with standard deviations